

U.S. Department of Energy

Idaho Operations Office • Idaho National Engineering Laboratory

**Cracking and Relocation of UO₂ Fuel
During Initial Nuclear Operation**

**Anthony D. Appelhans
Sig J. Dagbjartsson
Richard W. Miller**

120555031837 2 ANR3
US NRC
SECY PUBLIC DOCUMENT ROOM
BRANCH CHIEF
HST LOBBY
WASHINGTON DC 20555

May 1980

80 07810255

Prepared for the
U.S. Nuclear Regulatory Commission
Under DOE Contract No. DE-AC07-78IDO1570

 **EG&G** Idaho

NOTICE

This report was prepared as an account of work sponsored by an agency of the United States Government. Neither the United States Government nor any agency thereof, nor any of their employees, makes any warranty, expressed or implied, or assumes any legal liability or responsibility for any third party's use, or the results of such use, of any information, apparatus, product or process disclosed in this report, or represents that its use by such third party would not infringe privately owned rights.

Available from

GPO Sale Program
Division of Technical Information and Document Control
U.S. Nuclear Regulatory Commission
Washington, D.C. 20555

and

National Technical Information Service
Springfield, Virginia 22161

CRACKING AND RELOCATION OF UO₂ FUEL DURING INITIAL NUCLEAR OPERATION

Anthony D. Appelhans
Sig J. Dagbjartsson^a
Richard W. Miller

Published May 1980

EG&G Idaho, Inc.
Idaho Falls, Idaho 83415

Prepared for the
U.S. Nuclear Regulatory Commission
Washington, D.C. 20555
Under DOE Contract No. DE-AC07-76IDO1570
FIN No. A6041

a. On assignment for Gesellschaft Für Kernforschung, West Germany.

ABSTRACT

Long-term irradiations of instrumented fuel assemblies at the Heavy Boiling Water Reactor in Halden, Norway are being managed by EG&G Idaho, Inc., for the Nuclear Regulatory Commission. One of these instrumented fuel assemblies, IFA-430, was used to study fuel cracking and relocation during initial nuclear operation.

The threshold power at which pellet cracking and relocation is complete during the first power ramp and the effects of fabricated fuel-cladding gap size and power ramp rate on the threshold power value were determined from fuel rod axial gas flow data. No significant cracking or relocation was found to occur during the second, third, or fourth power ramps.

SUMMARY

Cracking and relocation of light water reactor (LWR) fuel pellets affect the axial gas flow path within nuclear reactor fuel rods and the thermal performance of the fuel. As part of the Nuclear Regulatory Commission's Water Reactor Safety Research Fuel Behavior Program, the Thermal Fuels Behavior Program of EG&G Idaho, Inc., is conducting fuel rod behavior studies in the Heavy Boiling Water Reactor in Halden, Norway. The Instrumented Fuel Assembly-430 (IFA-430) operated in that facility is a multipurpose assembly designed to provide information on fuel cracking and relocation, the long-term thermal response of LWR fuel rods subjected to various internal pressures and gas compositions, and the release of fission gases.

This report presents the results of an analysis of fuel cracking and relocation phenomena as deduced from fuel rod axial gas flow and fuel temperature data from the first four power ramps of the IFA-430 tests. Other axial gas flow experiments performed to date have been out-of-core tests on high burnup fuel rods and tests using simulated fuel pellets in unirradiated rods; the objective of this study is to investigate fuel cracking and relocation using axial gas flow and fuel temperature measurements acquired during irradiation.

The IFA-430 contains four, 1.28-m-long fuel rods loaded with 10% enriched UO_2 pellet fuel. Two of the rods, termed thermocouple rods, are each equipped with two centerline and three off-center thermocouples. These rods are prepressurized to 0.48 MPa with helium and are equivalent in design except for the fuel-cladding gap size; one rod has a fabricated gap size of 100 μm and the other 230 μm . The remaining two rods, termed gas flow rods, are each instrumented with a centerline thermocouple and three axially spaced pressure sensors and are equivalent in design except for gap size (100 and 230 μm).

The gas flow rods are connected, top and bottom, to a system that allows gas to be forced through the rods. The gas flow system and fuel rod pressure sensors provide a means for determining the hydraulic diameter (for axial gas flow) in the rods. Gas flow tests are conducted using two different procedures; steady state and transient

gas flow. The steady state gas flow tests are performed by establishing a steady flow of gas through the gas flow rods; the transient gas flow tests are performed by first pressurizing the gas flow rods and then opening a fast-acting valve, allowing the rod to depressurize. Both types of gas flow tests are performed during periods of constant reactor power. The first two weeks of nuclear operation of IFA-430 consisted of four, staircase-type power ramps. Steady state and transient gas flow tests were performed at each of the power levels during the power ramps to determine the hydraulic diameter; fuel temperature measurements were made at 15-minute intervals.

Changes in the hydraulic diameter during operation of the fuel are indications of cracking and relocation of fuel pellets. The hydraulic diameter is a measurement of the resistance to flow; cracked and relocated fuel pellet fragments result in a more tortuous flow path (hence, higher flow resistance) than that associated with uncracked pellets. The hydraulic diameter of the fuel rod is determined by measuring the pressure drop along the rod.

The temperature of the fuel, both at centerline and off-center locations within the pellet, also provides an indication of fuel pellet cracking and relocation. Radial (diametral) cracks decrease the fuel-cladding gap size and result in lower fuel temperatures. Azimuthal (circumferential) cracks decrease the effective fuel thermal conductivity, resulting in increased fuel temperature.

Previously developed methods were used to analyze the steady state gas flow test data, and new analysis methods were developed for analyzing the transient gas flow data. The transient gas flow analysis technique permits determination of the fuel rod hydraulic diameter using only the fuel rod plenum depressurization data.

The results of the gas flow and fuel temperature analyses indicate that cracking and relocation occur during the first power ramp up to a threshold power level, above which further cracking and relocation are insignificant. During the remaining ramps, no further significant cracking or relocation occur. The relocation threshold exhibits a dependence on fabricated fuel-cladding

gap size and on ramp rate. The fuel cracking during the lower power period of the first power ramp confirms the theoretical hypothesis that the fuel should crack at powers of ~ 5 kW/m during the

first power ramp, but the data also show that cracking and relocation continue to occur up to powers of ~ 20 kW/m.

ACKNOWLEDGMENTS

The authors gratefully acknowledge the Halden Project Staff for their support and cooperation, G. S. Reilly for processing and preparing the data, and R. R. Hobbins for his review and consultation. Appreciation is also expressed to W. F. Domenico and D. H. Malin for their work on Appendix E; to D. W. Brite and C. R. Hahn of

Battelle Pacific Northwest Laboratories for providing the fuel fabrication and characterization data contained in that appendix; and to Knut Lunde, metallurgist at the Kjeller Metallurgical Laboratory, Kjeller, Norway, for his work on Appendix F.

CONTENTS

ABSTRACT	ii
SUMMARY	iii
ACKNOWLEDGMENTS	v
1. INTRODUCTION	1
2. EXPERIMENT DESIGN AND CONDUCT	3
3. ANALYTICAL TECHNIQUES	10
3.1 Steady State Gas Flow	10
3.2 Transient Gas Flow	10
4. EXPERIMENT RESULTS	13
4.1 Gas Flow Results	13
4.2 Fuel Temperature Results	13
5. FUEL BEHAVIOR	19
5.1 Cracking and Relocation During the Initial Power Ramp	19
5.2 Cracking and Relocation Following the Initial Power Ramp	21
6. CONCLUSIONS	25
7. REFERENCES	26
NOTE: All of the appendices to this report are presented on microfiche attached to the inside of the back cover.	
APPENDIX A—IFA-430 POWER CALIBRATION	27
APPENDIX B—DESCRIPTION OF TEST CONDUCT AND DETAILED GAS FLOW DATA	31
APPENDIX C—STARTUP PERIOD DATA PLOTS	43
APPENDIX D—IFA-430 INSTRUMENTATION	45
APPENDIX E—IFA-430 FUEL AND CLADDING FABRICATION	67
APPENDIX F—FUEL ROD FABRICATION	99

FIGURES

1.	Isometric of IFA-430	4
2.	IFA-430 instrumentation locations	5
3.	Location of fuel centerline and off-center thermocouples in thermocouple rods (Rods 1 and 3)	6
4.	Location of fuel centerline thermocouple and rod pressure sensors in gas flow rods (Rods 2 and 4)	7
5.	Simplified schematic of IFA-430 gas flow system	8
6.	IFA-430 fuel rod power history during initial irradiation period	9
7.	Typical plenum pressure decay curve for small gap rod with corresponding best fit line, $Q \propto t$	12
8.	Comparison of hydraulic diameters, D_H , determined from steady state and transient gas flow tests for the first power ramp	12
9.	Rod 2 internal pressure drop for steady state flow of 18.6 and 40 L/min at rod average power of 33 kW/m and relative axial power profile	14
10.	Rod 4 internal pressure drop for steady state flow of 2 and 3.5 L/min at rod average power of 33 kW/m	14
11.	Rod pressure decay at three axial locations during transient depressurization test at rod average power of 29 kW/m (P_3 = plenum, P_2 = middle, P_1 = bottom)	15
12.	Rod pressure decay at three axial locations during transient depressurization test at rod average power of 31 kW/m (P_6 = plenum, P_5 = middle, P_4 = bottom)	15
13.	Centerline temperature of large gap gas flow rod (Rod 2) during first power ramp up	16
14.	Centerline temperature of small gap gas flow rod (Rod 4) during first power ramp up	16
15.	Lower centerline and one off-center temperature of small gap thermocouple rod (Rod 3) during first power ramp up	17
16.	Comparison of fuel centerline temperatures measured in the Gap Conductance Tests with fuel temperatures measured in the IFA-430 Tests	18
17.	Comparison of fuel off-center temperatures measured in the Gap Conductance and IFA-430 Tests	18
18.	Average hydraulic diameter, D_H , for the total rod versus average rod power for the first power ramp up and down and FRAP-T5 calculated gap	20
19.	Hoop stress and UO_2 fracture stress as a function of power for IFA-430 design pellet	20

20.	Gas flow rod sections and relative axial power profile for IFA-430 fuel rods	21
21.	Average hydraulic diameter, D_H , of the top section of Rods 2 and 4 as a function of section average power for the first power ramp up and down	22
22.	Average hydraulic diameter, D_H , of the middle section of Rods 2 and 4 as a function of section average power for the first power ramp up and down	22
23.	Lower centerline temperature and local power of large gap gas flow rod (Rod 2) during first power ramp up	23
24.	Centerline temperature and local power of small gap gas flow rod (Rod 4) during first power ramp up	23
25.	Hydraulic diameter extrapolated to zero power for the first four power ramps and prior to irradiation	24
26.	Upper centerline temperature of small gap thermocouple rod (Rod 3) at 10 and 20 kW/m local power during each power ramp	24
27.	Upper centerline temperature of small gap thermocouple rod (Rod 3) during first power ramp up	24
A-1.	IFA-430 neutron detector axial and radial locations (axial locations measured in mm from core bottom plate)	30
B-1.	Approximate periods during the first four power ramps of IFA-430 when steady state and transient gas flow tests were performed	34
B-2.	IFA-430 gas flow system schematic	35
C-1. through C-77.	Fuel temperature versus power for first four power ramps	43
C-78. through C-112.	Fuel temperatures and power as a function of time for first four power ramps	43
D-1.	IFA-430 test assembly and instrument identification	48
D-2.	Location of fuel centerline and off-center thermocouples in thermocouple rods (Rods 1 and 3)	49
D-3.	Location of fuel centerline thermocouples and rod pressure sensors in gas flow rods (Rods 2 and 4)	50
D-4.	Typical Halden fuel centerline thermocouple wiring illustration	51
D-5.	Illustration of IFA-430 fuel pellet drilling for centerline and off-center thermocouples	52
D-6.	IFA-430 fuel rod pressure transducer and gas flow lines	53

D-7.	IFA-430 gas flow system schematic	54
D-8.	IFA-430 neutron detector axial and radial locations (axial locations measured in mm from core bottom plate)	55
D-9.	Typical neutron detector	56
D-10.	Typical vanadium neutron detector reference signal versus time	57
D-11.	Calibration valve illustration	58
D-12.	Steam sampler in upper section of IFA-430	59
D-13.	Turbine flowmeter schematic	60
D-14.	Pressure transducer schematic	61
D-15.	Pressure transducer calibration curves for P152, P153, and P161	62
D-16.	Typical differential pressure flowmeter schematic	63
D-17.	Differential pressure transducer schematic	64
D-18.	Pipe dimensions and volumes for critical segments of IFA-430 gas flow system	65
E-1.	Fuel material flow chart	70
E-2.	Process flow chart	72
E-3.	Visual standards for UO ₂ fuel pellets	73
E-4.	IFA-430 fuel pellet dimensional and density specification	74
E-5.	Influence of pellet density on change during resintering	88
E-6.	Thermal resistivity of 95% TD stable fuel before and after heat treatment near 1600°C	90
E-7.	Thermal conductivity of 95% TD fuel and comparable NRC reference data	91
F-1.	Fabrication flow chart for Rods 1 and 3	102
F-2.	Fabrication flow chart for Rods 2 and 4	103
F-3.	Fabrication flow chart for Rods 2 and 4 (continued)	104
F-4.	Pellet positions for Rods 1 and 3	105
F-5.	Pellet positions for Rods 2 and 4	106
F-6.	Inside diameter measurement for Rod 1	108
F-7.	Inside diameter measurement for Rod 3	109
F-8.	Inside diameter measurement for Rod 2	110

F-9.	Inside diameter measurement for Rod 4	111
F-10.	Outer diameter of cladding tube, Rod 1, at 50-mm intervals for 0- and 90-degree orientations	112
F-11.	Outer diameter of cladding tube, Rod 2, at 50-mm intervals for 0- and 90-degree orientations	113
F-12.	Outer diameter of cladding tube, Rod 3, at 50-mm intervals for 0- and 90-degree orientations	114
F-13.	Outer diameter of cladding tube, Rod 4, at 50-mm intervals for 0- and 90-degree orientations	115
F-14.	Bottom end plug with fuel and thermocouples, Rod 1	117
F-15.	Bottom end plug with fuel and thermocouples, Rod 3	117
F-16.	Rods 1 and 3 length measurements	119
F-17.	Rods 2 and 4 length measurements	120

TABLES

1.	IFA-430 Fuel Rod Instrumentation and Design Variables	9
B-1.	Steady State Gas Flow Test Pressures and Flow Rates	36
D-1.	Neutron Detector Sensitivities	56
D-2.	Turbine Flowmeter Measurement Inaccuracies	60
D-3.	IFA-430 Gas Flowmeter Operating Ranges	65
E-1.	Fuel Pellet Inspections	71
E-2.	IFA-430 Fuel Pellet Impurity Specifications	75
E-3.	UO ₂ Powder Properties	76
E-4.	IFA-430 Process Parameters	77
E-5.	IFA-430 Powder Analysis	78
E-6.	Green Pellet Data for IFA-430	79
E-7.	IFA-430 Final Pellet Inspection Summary	80
E-8.	Comparison of Fabrication Characteristics of IFA-430 Fuel with PNL 95% TD Stable Fuel	81
E-9.	Comparison of Specific Impurities of IFA-430 Fuel with PNL 95% TD Stable Fuel	82

E-10.	Pore Distribution in PNL 95% Stable Fuel	83
E-11.	Grain Size of As-Sintered Pellets and Pellets Following 1875- and 1975-K/24-h Resintering Tests	84
E-12.	Resintering Test Conditions	85
E-13.	Results of 1875-K/24-h and 1975-K/7.8-h Resintering Tests	85
E-14.	Results of Resintering Tests	86
E-15.	Summary of Results of Resintering Tests	88
E-16.	Summary of Thermal Treatment and Resulting Changes in Thickness, Resistivity, and Density	89
E-17.	Coefficients for First- and Second-Order Equations Fit to Thermal Resistivity Data	90
E-18.	Summary of Instrumentation Hole Diameter Measurements	92
E-19.	IFA-430 Cladding Traceability Information	93
E-20.	IFA-430 Finished Cladding Characterization	94
E-21.	IFA-430 Cladding Chemical Analysis	95
E-22.	IFA-430 Ingot Characterization	96
E-23.	IFA-430 Extruded Tube Characterization	97
F-1.	Pellet Density Measurements	107
F-2.	Moisture Content of Reference Pellets from IFA-430	117
F-3.	Free Volume Measurements	121

CRACKING AND RELOCATION OF UO₂ FUEL DURING INITIAL NUCLEAR OPERATION

1. INTRODUCTION

A major objective of the United States Nuclear Regulatory Commission's Reactor Safety Research Program¹ is to establish analytical codes capable of predicting commercial nuclear fuel performance for a wide range of operating conditions which could occur during the life of a light water reactor (LWR) fuel rod. An extensive fuel behavior research program has been implemented in which in-pile and out-of-pile experiments are conducted to study fuel rod responses to normal and abnormal operating conditions.

Included in this program are studies of uranium oxide and mixed oxide fuel behavior performed at the Heavy Boiling Water Reactor (HBWR) in Halden, Norway. The HBWR was built by the Norwegian Institutt for Atomenergi, and has been operated by the Organization for Economic Cooperation and Development (OECD) Halden Reactor Project through an international agreement between participating governments and organizations. One of the assemblies being irradiated in the HBWR is the Instrumented Fuel Assembly-430 (IFA-430) managed by EG&G Idaho, Inc., for the Nuclear Regulatory Commission. IFA-430 was designed to provide fuel rod axial gas flow, fuel temperature, and fission gas release data for LWR fuel rods.

The purpose of this report is to present the results of an analysis of fuel cracking and relocation phenomena using data from the first four power ramps of the IFA-430. The cracking and relocation of fuel pellets affects the thermal performance of the fuel. Cracking of the fuel pellets and relocation of the fuel into the fuel-cladding gap alters the effective fuel thermal conductivity (in the case of circumferential cracks) and the pellet-to-cladding gap; both of these phenomena affect the stored energy in the fuel and, therefore, the behavior of the fuel during operational changes. The times at which the fuel cracks (at what power) and at which cracking and relocation are essentially complete are important in the design of fuel behavior experiments.

The IFA-430 consists of four, LWR-type fuel rods. Two rods (Rods 1 and 3), with diametral gap sizes of 100 and 230 μm , respectively, are pressurized to 0.48 MPa with helium and instrumented with centerline and off-center fuel thermocouples. These two rods are termed thermocouple rods. Each of the other two rods (Rods 2 and 4), termed gas flow rods, has three axially distributed pressure transducers mounted directly to the cladding, a centerline thermocouple, and each is connected to an external gas supply system that allows gas to be forced through the rod. Rods 2 and 4 have the same diametral gap sizes as Rods 1 and 3, respectively. The gas flow system and axial pressure transducers provide a means for quantifying the axial gas flow through the fuel rods.

The IFA-430 is unique in that it provides the opportunity to investigate the relationship of axial gas flow and fuel temperature measurements performed during nuclear operation to fuel pellet cracking and relocation. Other axial gas flow experiments have included out-of-core tests on high burnup fuel rods² and on unirradiated fuel rods with simulated fuel pellets³. Axial gas flow data from the initial operation of the IFA-430 fuel provides insight into when the fuel pellets crack and how the fuel behaves (relocates) after cracking.

The temperature behavior of the fuel, both at the centerline and off-center locations, also provides insight to the amount of cracking and relocation that has occurred. In IFA-430 the fuel temperatures are obtained by thermocouple configurations similar to those used in the Gap Conductance Test Series,⁴ conducted in the Power Burst Facility at the Idaho National Engineering Laboratory, to allow comparison with the results of that test series.

During initial operation of IFA-430, measurement of the axial gas flow behavior of the gas flow rods was performed at a variety of steady state

reactor powers using both the steady state and transient gas flow methods. The steady state gas flow tests are performed by establishing a steady flow of gas through the gas flow rods; the transient gas flow tests are performed by first pressurizing the gas flow rods and then operating a fast-acting valve, allowing the rod to depressurize. The gas flow measurements permit calculation of the fuel rod hydraulic diameter, which is an indicator of the extent of fuel pellet cracking and relocation. The fuel temperature measurements were performed at 15-minute intervals during the initial operation of IFA-430. The gas flow measurement procedures and operation of the IFA-430 during the initial nuclear operating period are described in Section 2.

Previously developed methods used to analyze the steady state gas flow test data, and new analysis methods developed for analyzing the

transient gas flow data are presented in Section 3. The transient gas flow analysis technique permits determination of the fuel hydraulic diameter using only the fuel rod plenum depressurization data.

Selected experiment results are presented in Section 4. Fuel cracking and relocation which occur during the first power ramp of the fuel, the fuel behavior (with respect to cracking) during subsequent ramps, and the effect of fuel-cladding gap size on fuel cracking are discussed in Section 5. The conclusions are presented in Section 6.

Detailed discussions of the assembly power calibration, the test conduct, the assembly instrumentation, fuel fabrication and characterization, and the fuel rod fabrication are presented in the appendices. All of the appendices to this report are provided on microfiche attached to the inside of the back cover.

2. EXPERIMENT DESIGN AND CONDUCT

IFA-430 contains four fuel rods (1.28 m long) with 10% enriched UO_2 fuel pellets. The assembly is shown in Figure 1 and instrument locations are identified in Figure 2. Two of the rods, termed thermocouple rods, are each equipped with two centerline thermocouples and three off-center thermocouples, as shown in Figure 3. The other two rods, termed gas flow rods, in addition to having one centerline thermocouple each, have three axially distributed pressure transducers mounted directly to the cladding, as shown in Figure 4, to measure internal gas pressure. In the thermocouple rods, one centerline and the three off-center thermocouples are located 72 mm from the bottom of the fuel stack and the other centerline thermocouple is located 132 mm from the top of the fuel stack. The gas flow rods have one centerline thermocouple located 72 mm from the bottom of the fuel stack. The gas flow fuel rods are connected, top and bottom, to the system, shown in Figure 5, which can impose pressures to force gas axially through the rod. The system is capable of providing a wide range of flow rates, as well as introducing new gases and gas mixtures. Table 1 presents the IFA-430 fuel rod instrumentation and design variables. A complete description of the assembly and instrumentation is given in Appendix D (on microfiche attached to back cover).

Irradiation of the assembly began in November 1978. During the first four power cycles, the fuel temperatures were monitored and a series of gas flow measurements was performed at steady state rod powers. The fuel rod power history for the initial irradiation period (four power cycles) is shown in Figure 6.

Two different procedures are used in obtaining the gas flow measurements; (a) steady state gas flow tests, and (b) transient gas flow tests. The steady state and transient terminology is used only in reference to the mode of gas flow; both types of tests are performed at steady state reactor power levels.

The steady state gas flow tests were conducted by flowing helium gas through the gas flow rods (one rod at a time), recording the pressure drop along the rod at each of the three axial pressure sensors, and measuring the volumetric flow rate. A series of tests, with flow rates varying from 2 to 120 L/min (STP) at inlet pressures from ~ 0.1 to 7.6 MPa, was conducted at several steady state power levels during each power ramp.

Transient gas flow tests were conducted by first pressurizing the back pressure tank (not shown in Figure 1) to pressure P_2 and closing the outlet valves at the bottom of the two fuel rods. The fuel rod pressure was then increased to P_1 ($P_1 > P_2$) and the inlet valves at the top of the fuel rods were closed. The fast-acting valve at the bottom of one rod was then opened, allowing the rod to depressurize against the back pressure, P_2 . The other rod was then depressurized in the same manner. The pressure at each of the three axial pressure sensors was recorded as each rod depressurized. Transient tests were performed at several power levels during each power ramp. Typical pressures were $P_1 = 4.0$ MPa, with $P_2 = 1.0$ MPa; and $P_1 = 1.0$ MPa, with $P_2 = 0.1$ MPa. Detailed descriptions of the steady state and transient gas flow test procedures and results are given in Appendix B (on microfiche attached to back cover).

The fuel and assembly thermocouples were checked for consistency under isothermal conditions during pre-nuclear heatup. During periods of reactor operation, the fuel temperatures were recorded at 15-minute intervals. The upper centerline thermocouple in the large gap thermocouple rod (Rod 1) failed early in the first power ramp and the lower centerline thermocouple failed during the fourth power ramp. All other fuel thermocouples performed satisfactorily.

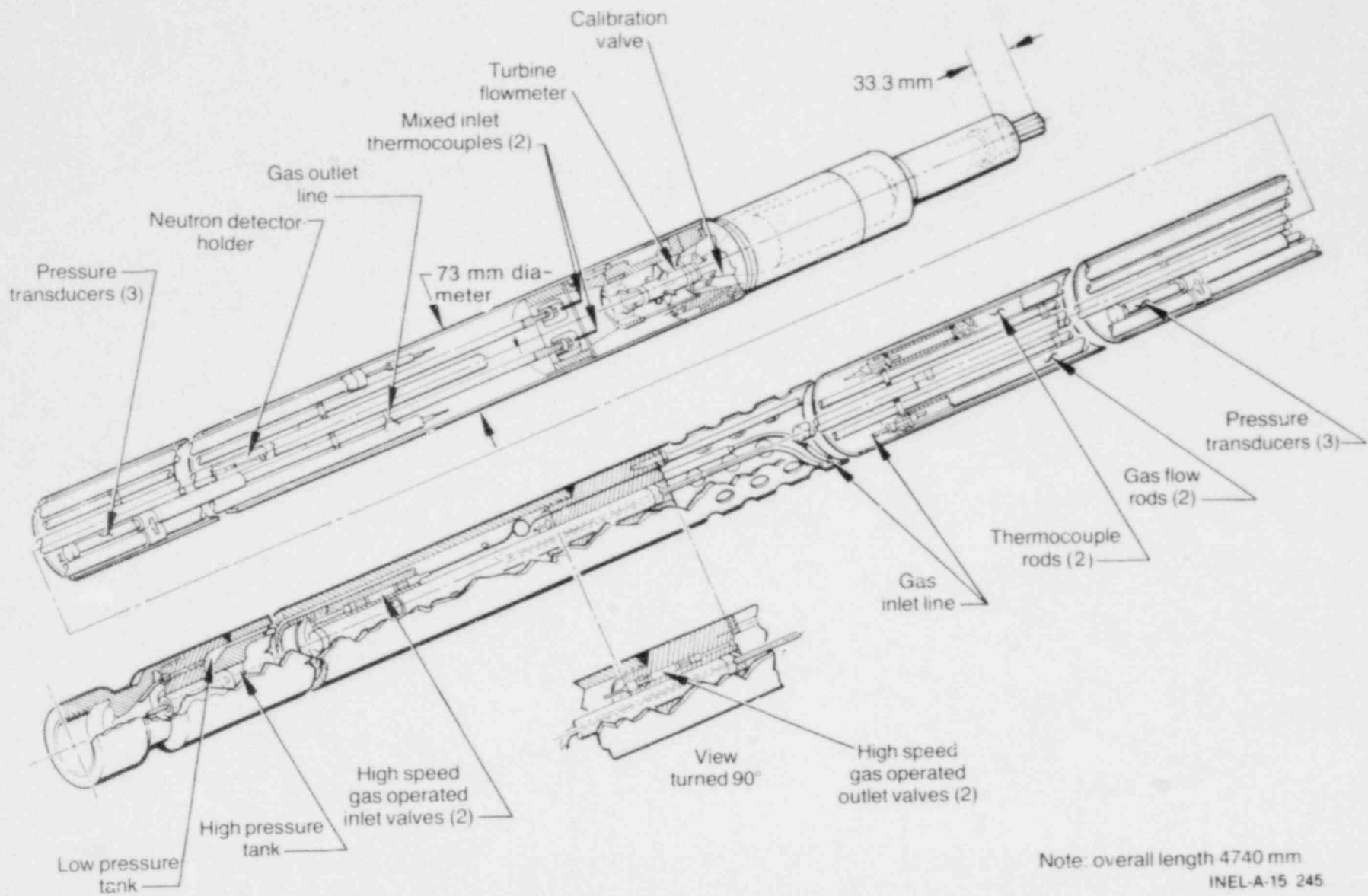


Figure 1. Isometric of IFA-430.

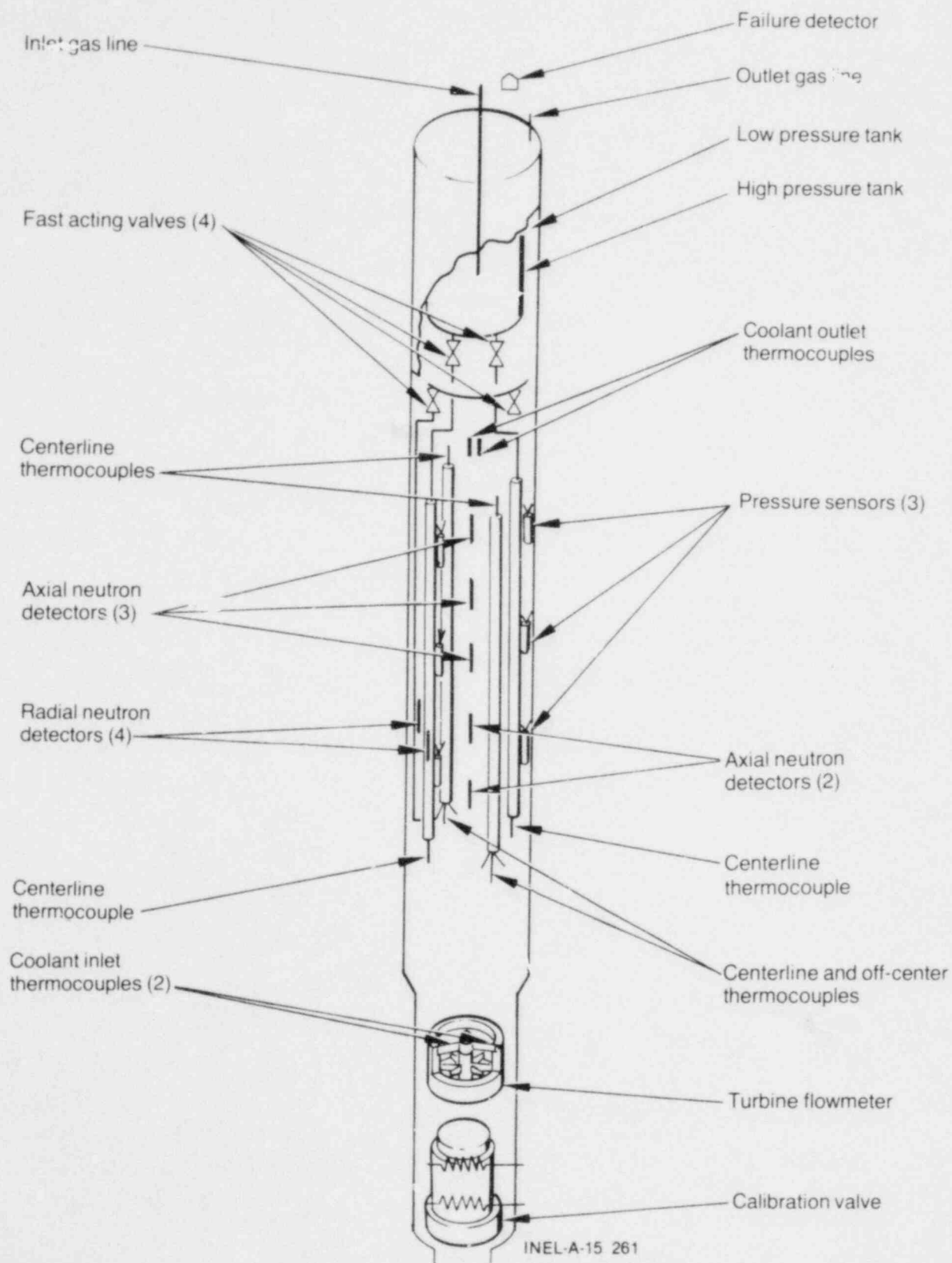


Figure 2. IFA-430 instrumentation locations.

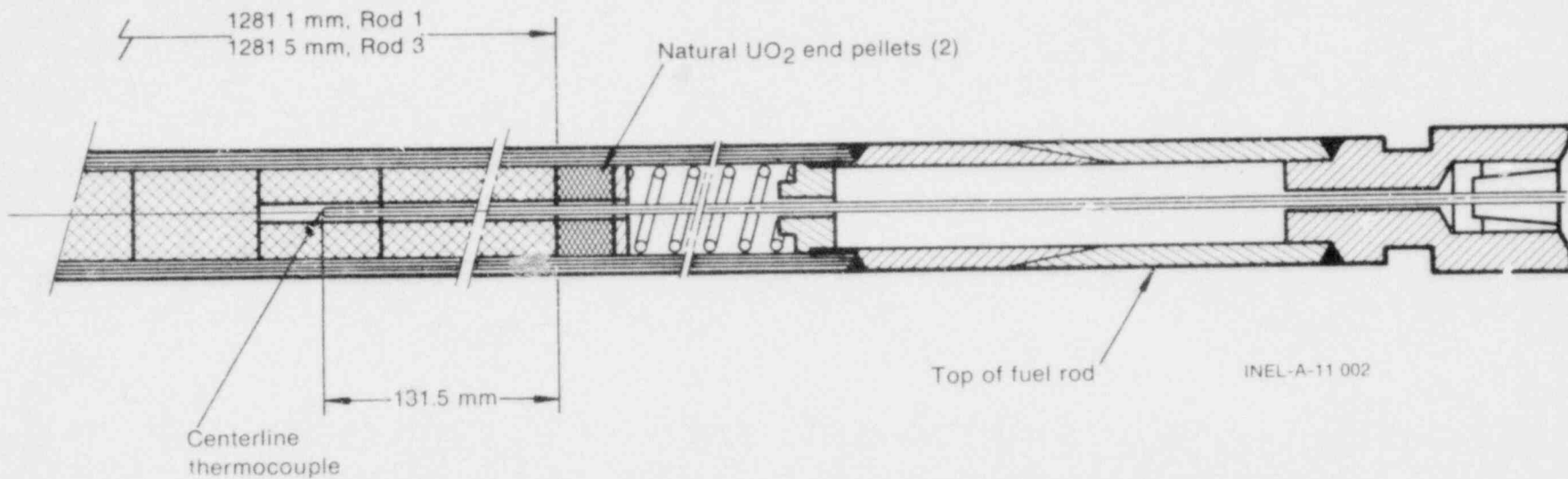
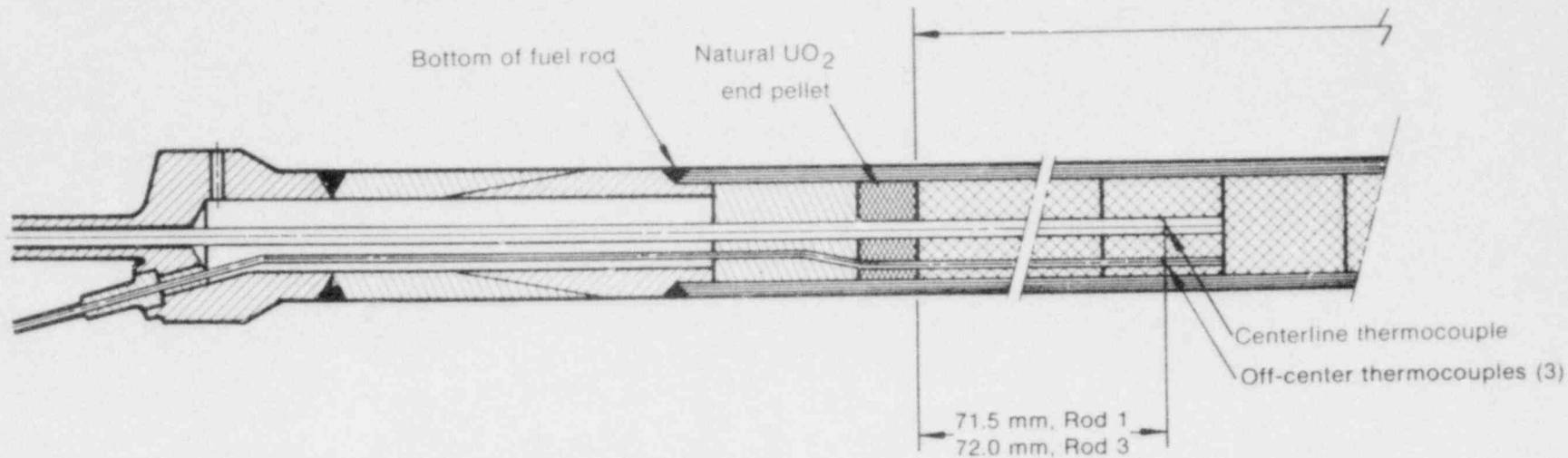
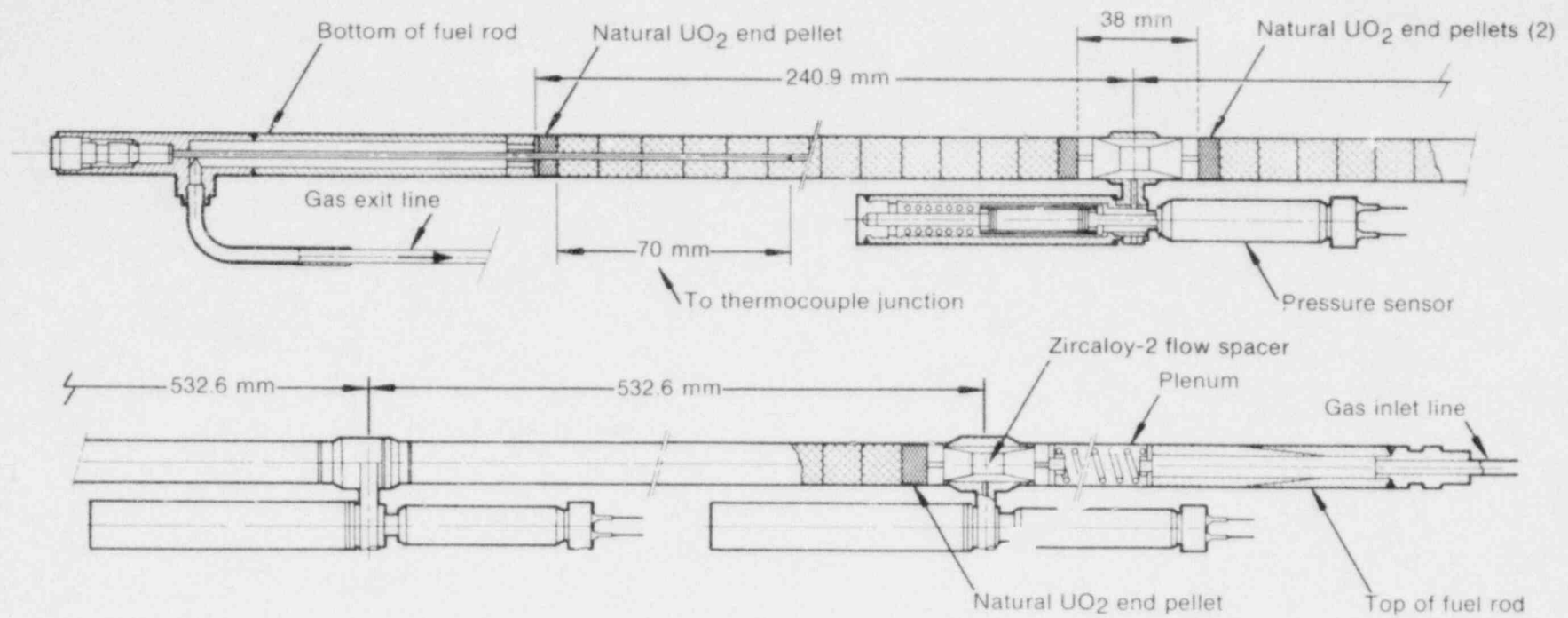


Figure 3. Location of fuel centerline and off-center thermocouples in thermocouple rods (Rods 1 and 3).



INEL-B-11 003

Figure 4. Location of fuel centerline thermocouples and rod pressure sensors in gas flow rods (Rods 2 and 4).

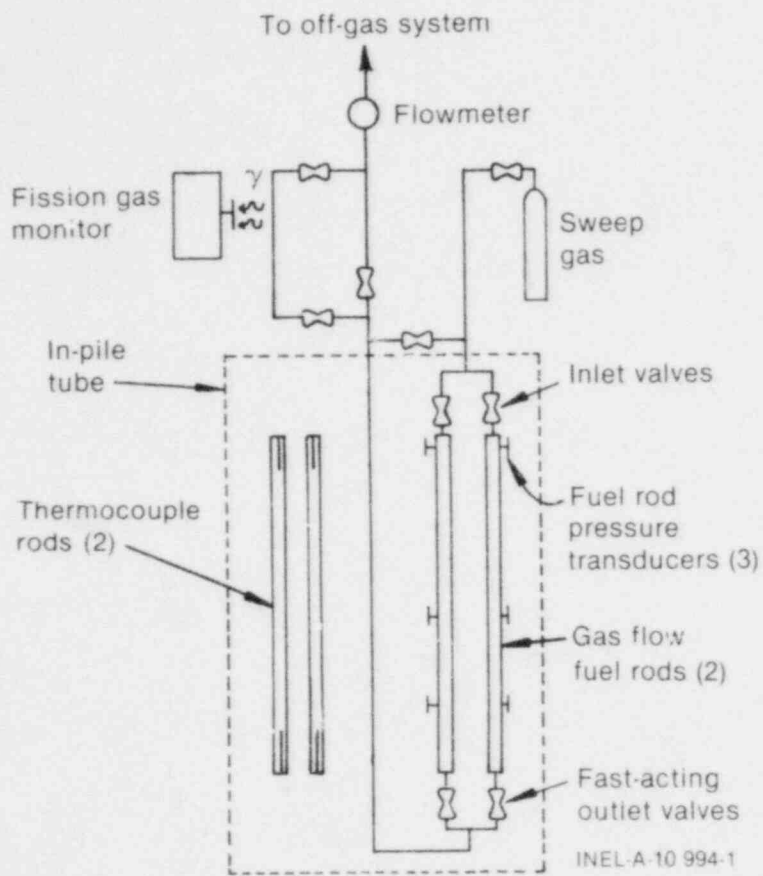


Figure 5. Simplified schematic of IFA-430 gas flow system.

Table 1. IFA-430 fuel rod instrumentation and design variables

Rod	Rod Type	Diametral Gap (mm)	Fill Gas	Instrumentation
1	Thermocouple	0.23	0.48 MPa He	Two centerline thermocouples, three off-center thermocouples
2	Gas flow	0.23	Variable	One centerline thermocouple, three pressure sensors
3	Thermocouple	0.10	0.48 MPa He	Two centerline thermocouples, three off-center thermocouples
4	Gas flow	0.10	Variable	One centerline thermocouple, three pressure sensors

Fuel:	Form	-	pressed and sintered UO ₂ pellets
	Enrichment	-	10 wt% ²³⁵ U
	Density	-	10.412 g/cm ³ (95% of theoretical)
	Shape	-	length, 12.7 mm
		-	diameter, ^a 10.81 mm, 10.68 mm
		-	ends, chamfered 45° to an approximate depth of 0.12 mm

Cladding: Zircaloy-2			
OD	-	12.79 mm	
ID	-	10.91 mm	

a. The pellet outside diameters are fabricated to give the two desired fuel-cladding gap sizes of 0.23 and 0.10 mm.

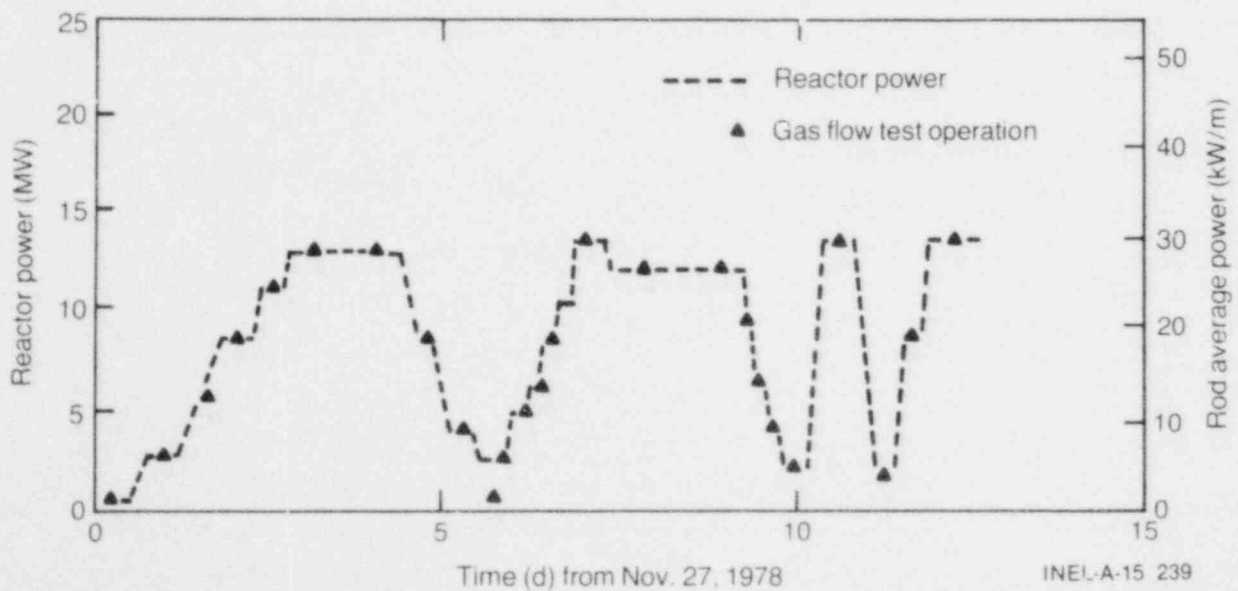


Figure 6. IFA-430 fuel rod power history during initial irradiation period.

3. ANALYTICAL TECHNIQUES

This section describes the analytical methods used to evaluate the gas flow test data with respect to cracking and relocation of the fuel.

The gas flow data are used to calculate an hydraulic diameter for axial gas flow through the fuel rod. The assumption is made for the analysis that the flow path consists of a regular annular gap between the fuel pellet column and the cladding. Deviations from this type of flow path, indicating fuel relocation, show up as a change in the calculated hydraulic diameter, which, in the case of an annular gap, is equivalent to the diametral gap size. Analytical techniques used to calculate the hydraulic diameter for the two gas flow rods from measured steady state and transient gas flow data are discussed in Section 3.1 below. The results of application of the analytical techniques to the data from IFA-430 are presented in Section 4 and are discussed in Section 5.

Gas flow data were obtained in the steady state and transient modes of operation as described in Section 2. For the analysis of these data, the basic gas flow equation⁵ correlating the laminar mass flow rate through an annular gap with measured pressures P_1 and P_2 along the flow path is used

$$\dot{m} = \frac{\pi \bar{D} D_H^3 (P_1^2 - P_2^2)}{Ha^2 RT \eta L} \quad (1)$$

where

- \dot{m} = mass flow rate (mol/s)
- \bar{D} = mean diameter between fuel surface and inside of cladding (m)
- D_H = hydraulic diameter (the diametral gap size for an annular gap) (m)
- η = gas viscosity (Pa·s)
- R = universal gas constant (J/K·mol)
- T = gas temperature (K)
- L = flow path length (m)

Ha = Hagen number (a measure of the friction between the gas and the gas path).

This equation describes steady state incompressible flow, where momentum and acceleration terms of the general momentum equation can be neglected.

3.1 Steady State Gas Flow

In the steady state mode of operation, the mass flow and the pressures P_1 and P_2 are measured. The geometrical constants D and L are known and the temperature of the gas in the gap is estimated from the cladding inside and the fuel surface temperatures. The Hagen number for a regular annular gap is used, along with its dependence on the gap size as observed by Reimann.⁵ Consequently, the only unknown in Equation (1) is the hydraulic diameter. Rearranging Equation (1) results in

$$D_H^3 = \frac{\dot{m} Ha^2 RT \eta L}{\pi \bar{D} (P_1^2 - P_2^2)} \quad (2)$$

from which the hydraulic diameter, D_H , is calculated.

3.2 Transient Gas Flow

The transient gas flow data consist of the rod plenum pressure as a function of time while the rod is allowed to depressurize against a back pressure. A method was developed to calculate the hydraulic diameter, D_H , using the plenum pressure decay and back pressure measurements.

The ideal gas law, applied to the pressure decay in the fuel rod upper plenum, results in

$$\frac{-dP_1}{dt} = \frac{RT}{V} \frac{dN}{dt} \quad (3)$$

where

P_1 = plenum pressure (Pa)

V = plenum volume (m³)

N = moles of gas in plenum.

Additionally, the decrease in the number of moles in the plenum with time is equal to the mass flow rate through the fuel rod [given by Equation (1)]. Equating dN/dt with the right hand side of Equation (1) and rearranging, results in the differential equation

$$\frac{-dP_1}{P_1^2 - P_2^2} = \frac{D_H^3 \pi \bar{D}}{Ha \eta L V} dt. \quad (4)$$

This differential equation, with the appropriate initial conditions, has the analytical solution

$$P_2 \frac{\pi \bar{D}}{Ha \eta L V} D_H^3 t = \log \left\{ \frac{[P_1(t) + P_2]/[P_1(t) - P_2]}{[P_1(0) + P_2]/[P_1(0) - P_2]} \right\}. \quad (5)$$

When the measured pressures in the upper plenum of the rod, P₁(t), are used to calculate the right hand side of Equation (5) and this quantity is plotted versus time, the points should fall on a straight line passing through the origin. Through least squares fit techniques this line can be represented as

$$\alpha t = \log \frac{[P_1(t) + P_2]/[P_1(t) - P_2]}{[P_1(0) + P_2]/[P_1(0) - P_2]} \quad (6)$$

where α now represents the slope of the best fit straight line passing through the origin. A typical

plenum pressure decay curve and the corresponding plot of Equation (6) are shown in Figure 7. Combining Equation (6) with Equation (5) gives

$$\alpha = P_2 \frac{D_H^3}{Ha \eta L V} \quad (7)$$

which can be rearranged to give the hydraulic diameter

$$D_H^3 = \frac{\alpha Ha \eta L V}{P_2 \pi \bar{D}} \quad (8)$$

Thus, both the steady state and transient gas flow data are used to calculate the hydraulic diameter, D_H. The steady state analysis technique uses the measured pressure drop along the rod and the mass flow rate, whereas the transient technique uses the measured pressure decay in the fuel rod plenum. The consistency of the two techniques is shown in Figure 8, in which the hydraulic diameters calculated using the steady state and transient gas flow data are compared. The disagreement between the hydraulic diameters determined by the two methods appears random with respect to power level and gap size, and is generally less than 15%. Part of the discrepancy could be due to the fact that the transient method involves the pressure drop across the entire rod length, whereas the steady state method involves the pressure drop between the plenum and the bottom pressure transducer, which is located 24 cm above the bottom of the fuel stack. Thus, the steady state method does not measure the hydraulic diameter in the bottom 24 cm of the fuel rod.

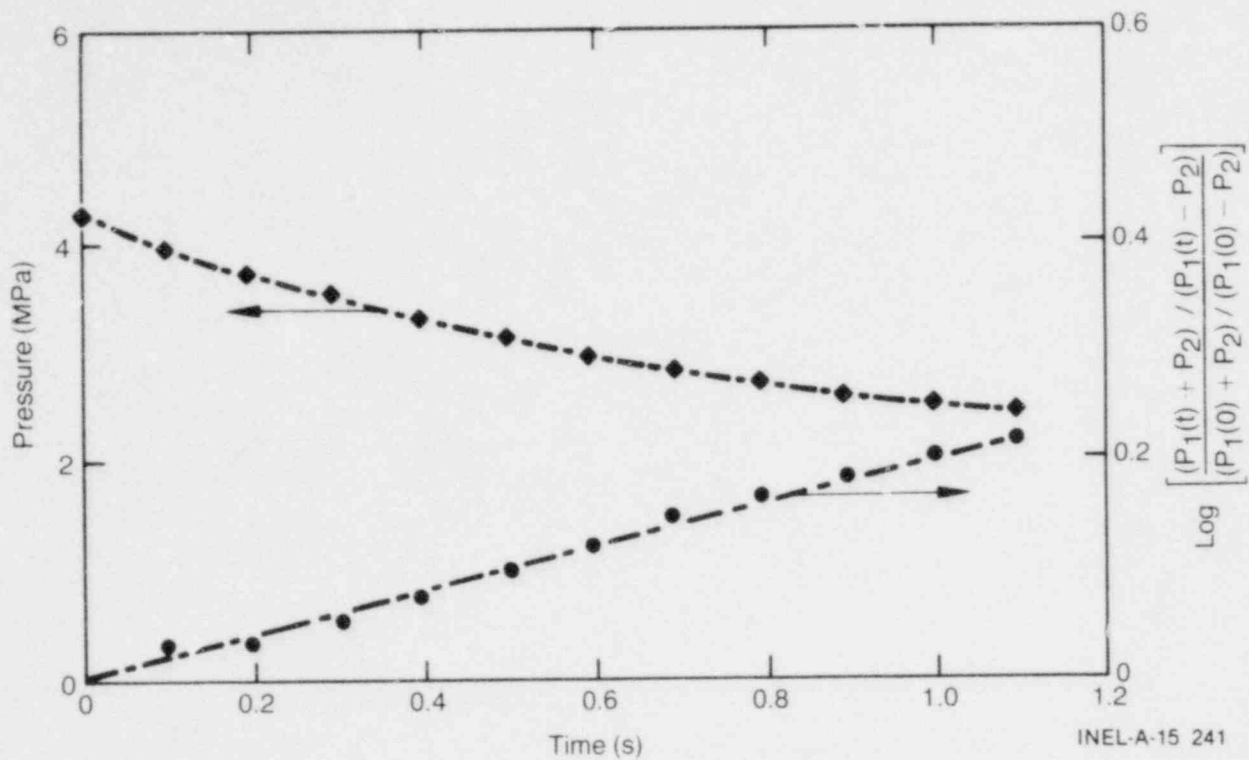


Figure 7. Typical plenum pressure decay curve for small gap rod with corresponding best fit line, $Q \propto t$.

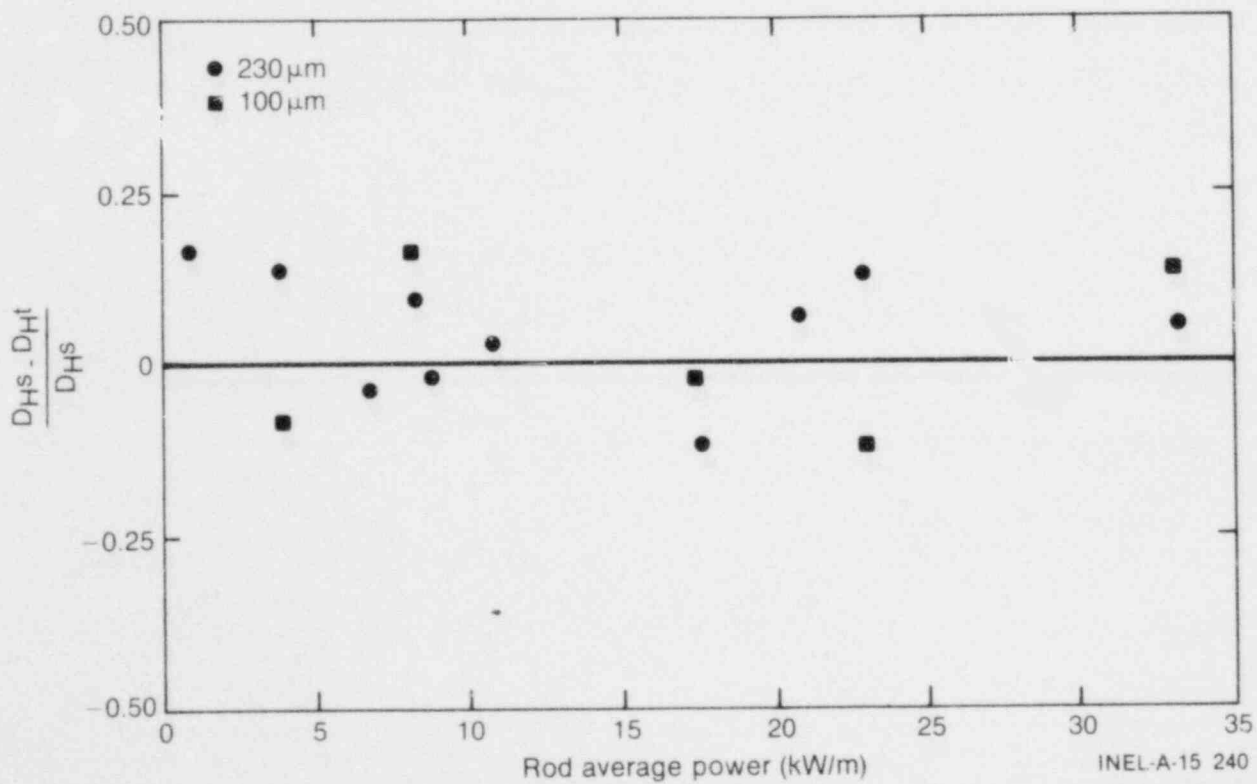


Figure 8. Comparison of hydraulic diameters, D_H , determined from steady state and transient gas flow test for the first power ramp.

4. EXPERIMENT RESULTS

Experiment data obtained during the startup period of the IFA-430 include: (a) gas flow data from which the hydraulic diameter of the fuel is determined and (b) fuel pellet centerline and off-center temperatures which provide an indication of fuel pellet cracking and relocation. The data were obtained during the first two weeks of nuclear operation of the assembly; the assembly experienced three up and down power ramps and a fourth power ramp up during the period.

This section presents selected gas flow data from steady state and transient gas flow tests, and fuel temperature measurements. Detailed plots of the individual fuel temperature measurements as a function of power and time for each of the power ramps are provided in Appendix C, and data for the gas flow tests are presented in Appendix B (both appendices are on microfiche attached to back cover). Discussion of the data and their application to fuel cracking and relocation is contained in Section 5.

4.1 Gas Flow Results

The hydraulic diameter of the fuel rods is calculated using the pressure drop along the rod and the mass flow rate data, and alternately with the fuel rod plenum depressurization data. The pressure drop and mass flow rate are measured at steady state gas flow conditions (steady state gas flow tests), and the fuel rod plenum depressurization is measured during transient gas flow conditions (transient gas flow tests). Typical examples of the pressure drop along the fuel rod and associated flow rate, along with the relative axial power profile of the rod, are shown in Figures 9 and 10. Qualitatively, the pressure drop is highest in the high power region of the rod (middle section) where the fuel temperature is high. Additionally, at the same inlet pressure, the flow rate in the large gap rod is significantly higher than in the small gap rod. Both of these effects were expected and indicate the instrumentation is operating properly.

Typical examples of the plenum depressurization data (transient gas flow tests) are shown in Figures 11 and 12; also included are the data from the fuel rod middle and bottom pressure sensors. Qualitatively, the pressure decay is dependent on the gap size and the average fuel rod power.

4.2 Fuel Temperature Results

The major characteristic of interest in the fuel temperature data for the first power ramp up is the behavior of the centerline temperatures in the gas flow rods. As shown in Figures 13 and 14, the fuel centerline temperature in the gas flow rods dropped in the 15- to 20-kW/m power range. The small gap thermocouple rod also showed a drop in centerline temperature, though slightly less than the gas flow rods, at about 17 kW/m, as shown in Figure 15.

The lower centerline and off-center temperature instrumentation in the large gap thermocouple rod appeared to malfunction during the first power ramp up and, as a result, they have not been used in the analysis and are not presented here. At present, the anomalous behavior during the first ramp has not been resolved; however, during the remaining power ramps the fuel temperature data (both off-center and centerline) for the large gap thermocouple rod appear normal (that is, the fuel temperatures are in the range expected and are similar to data from other tests⁴).

Fuel centerline and off-center temperatures for the fourth power ramp up are compared in Figures 16 and 17 with similar data collected during the Gap Conductance Test Series.⁴ The centerline temperatures measured in IFA-430 are slightly lower, for both the large gap and small gap rods, than those measured during the gap conductance tests. The off-center temperatures measured in IFA-430 for the large gap rod are generally slightly lower than those measured in the gap conductance tests and show similar scatter. However, the IFA-430 small gap rod off-center temperatures show more scatter and are slightly higher than the gap conductance test data.

A complete set of data for each thermocouple and each power ramp is contained in Appendix C (on microfiche attached to back cover). The centerline thermocouple (TF-1) located in the bottom of Rod 1 failed during the fourth power ramp up and the upper centerline thermocouple (TF-2) in Rod 1 failed during heatup prior to irradiation.

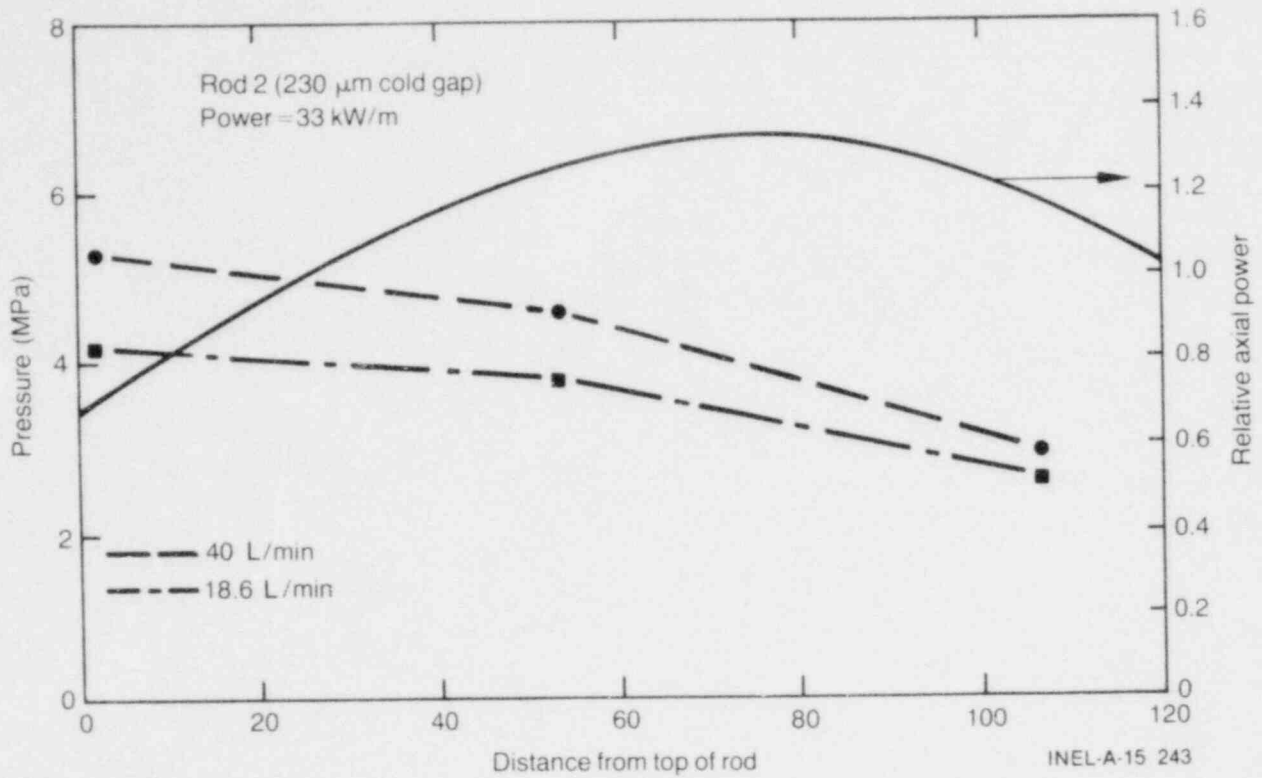


Figure 9. Rod 2 internal pressure drop for steady state flow of 18.6 and 40 L/min at rod average power of 33 kW/m and relative axial power profile.

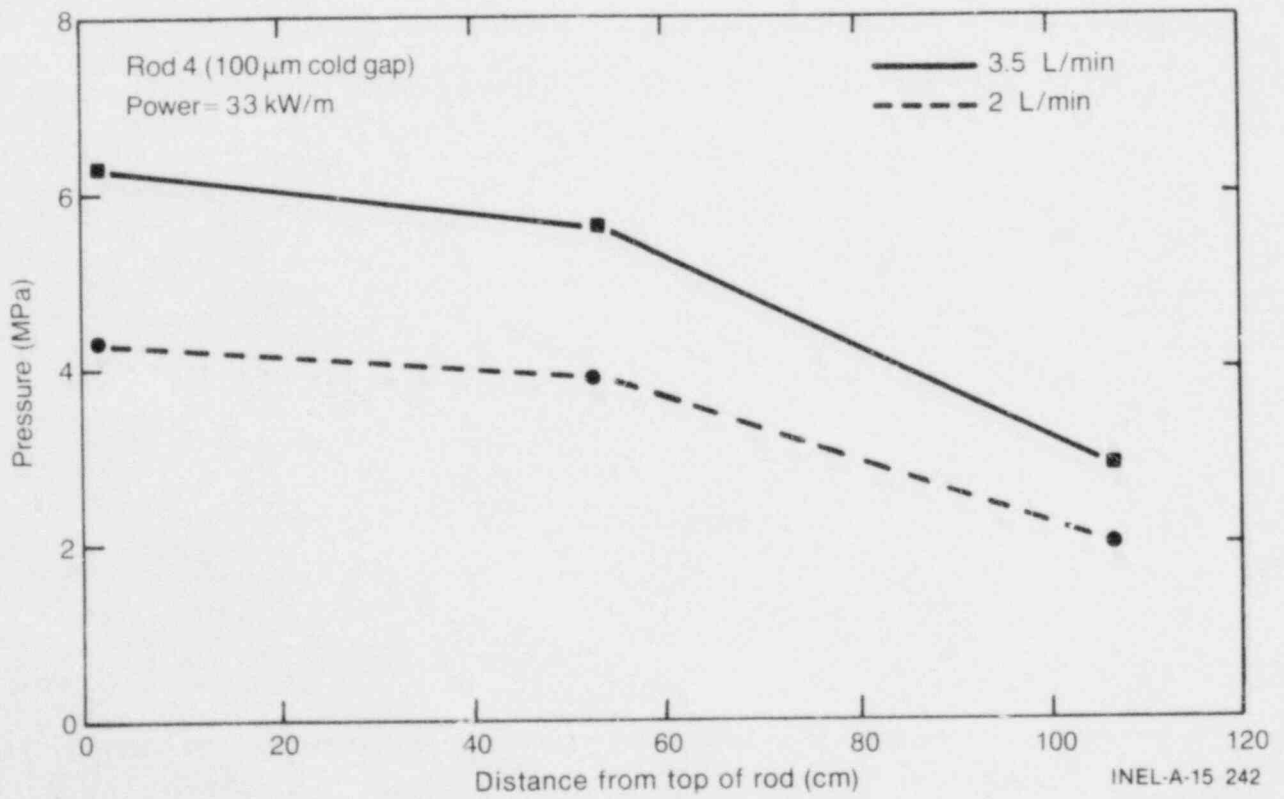


Figure 10. Rod 4 internal pressure drop for steady state flow of 2 and 3.5 L/min at rod average power of 33 kW/m.

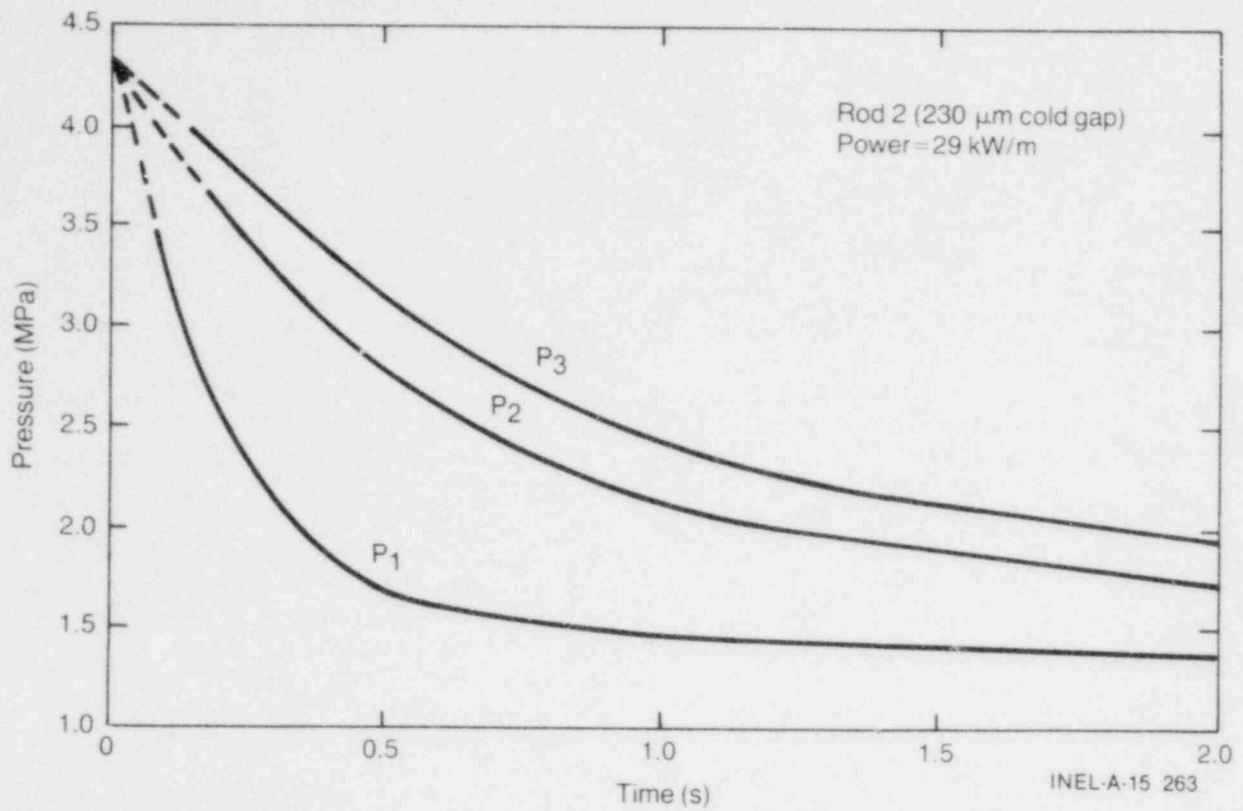


Figure 11. Rod pressure decay at three axial locations during transient depressurization test at rod average power of 29 kW/m (P_3 = plenum, P_2 = middle, P_1 = bottom).

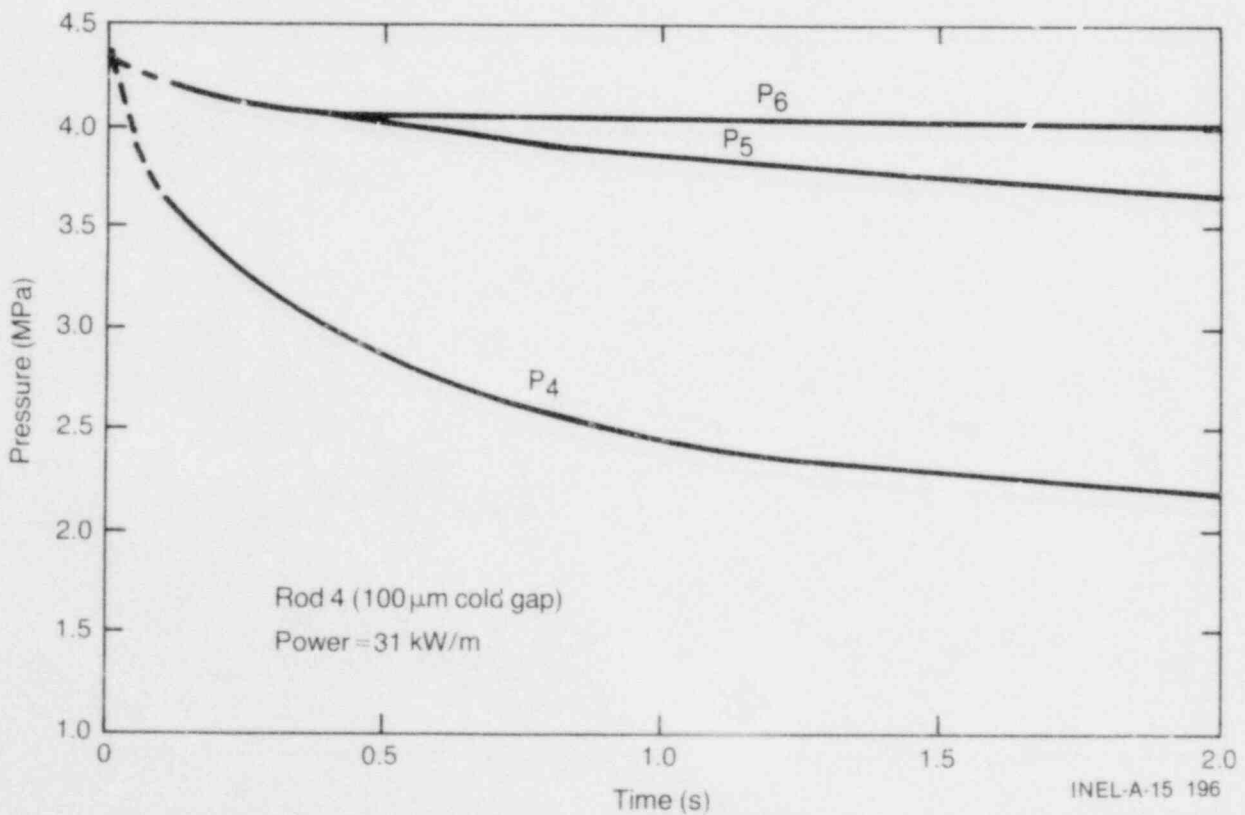


Figure 12. Rod pressure decay at three axial locations during transient depressurization test at rod average power of 31 kW/m (P_6 = plenum, P_5 = middle, P_4 = bottom).

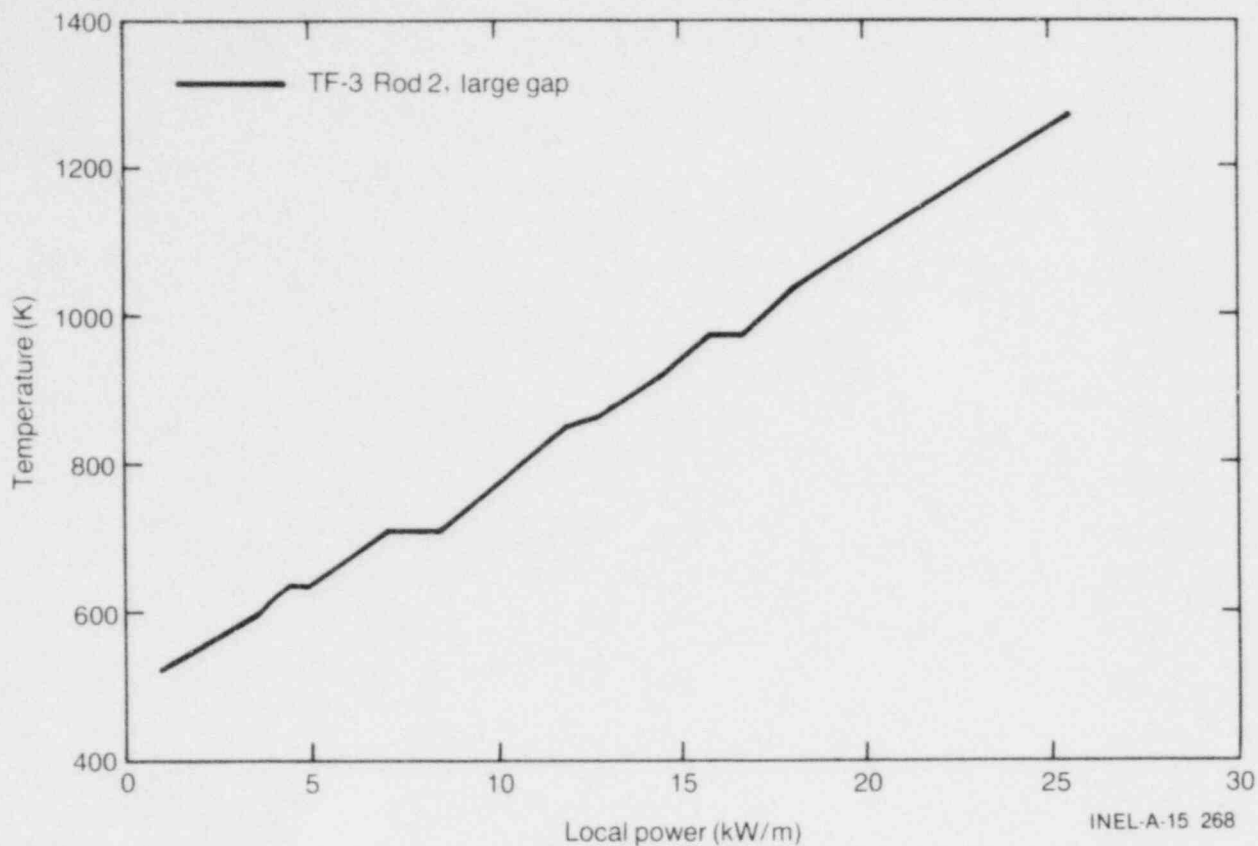


Figure 13. Centerline temperature of large gap gas flow rod (Rod 2) during first power ramp up.

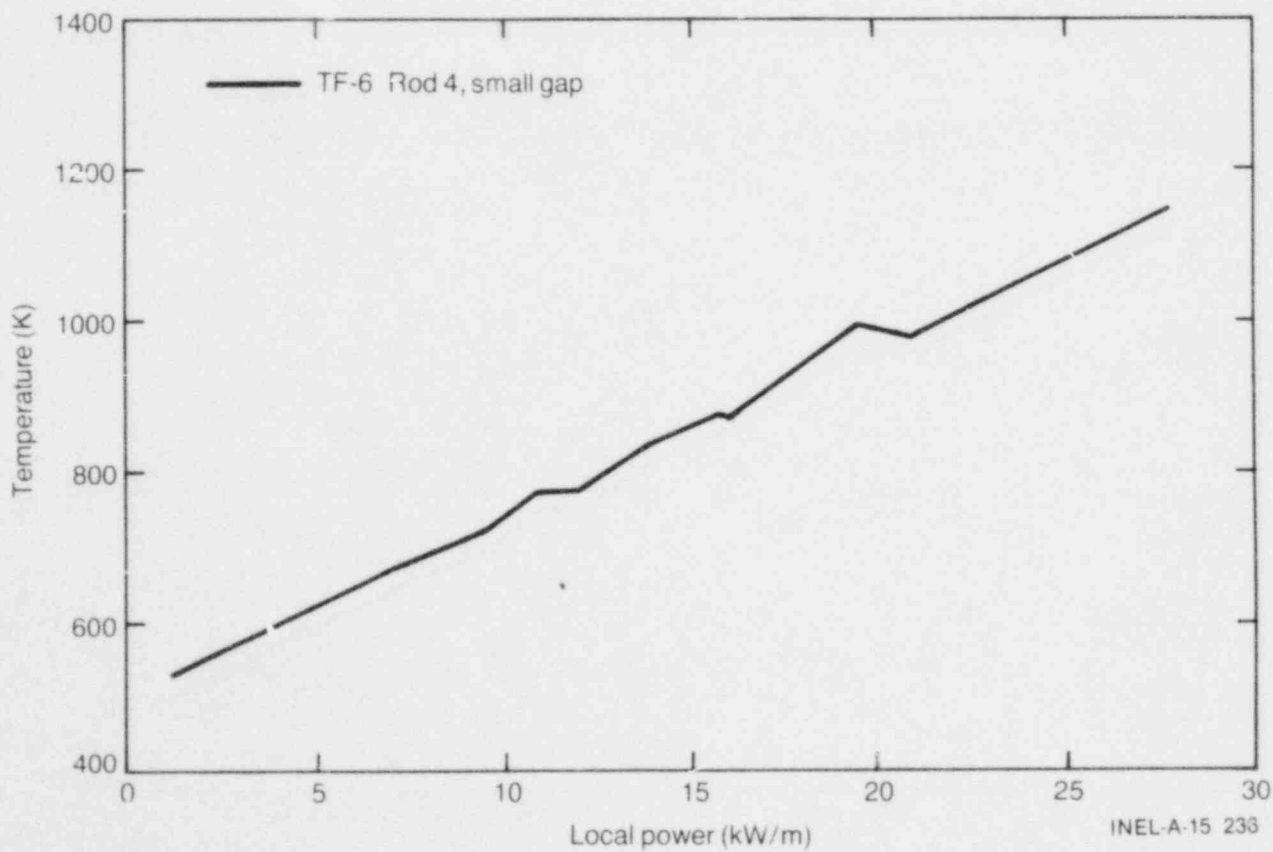


Figure 14. Centerline temperature of small gap gas flow rod (Rod 4) during first power ramp up.

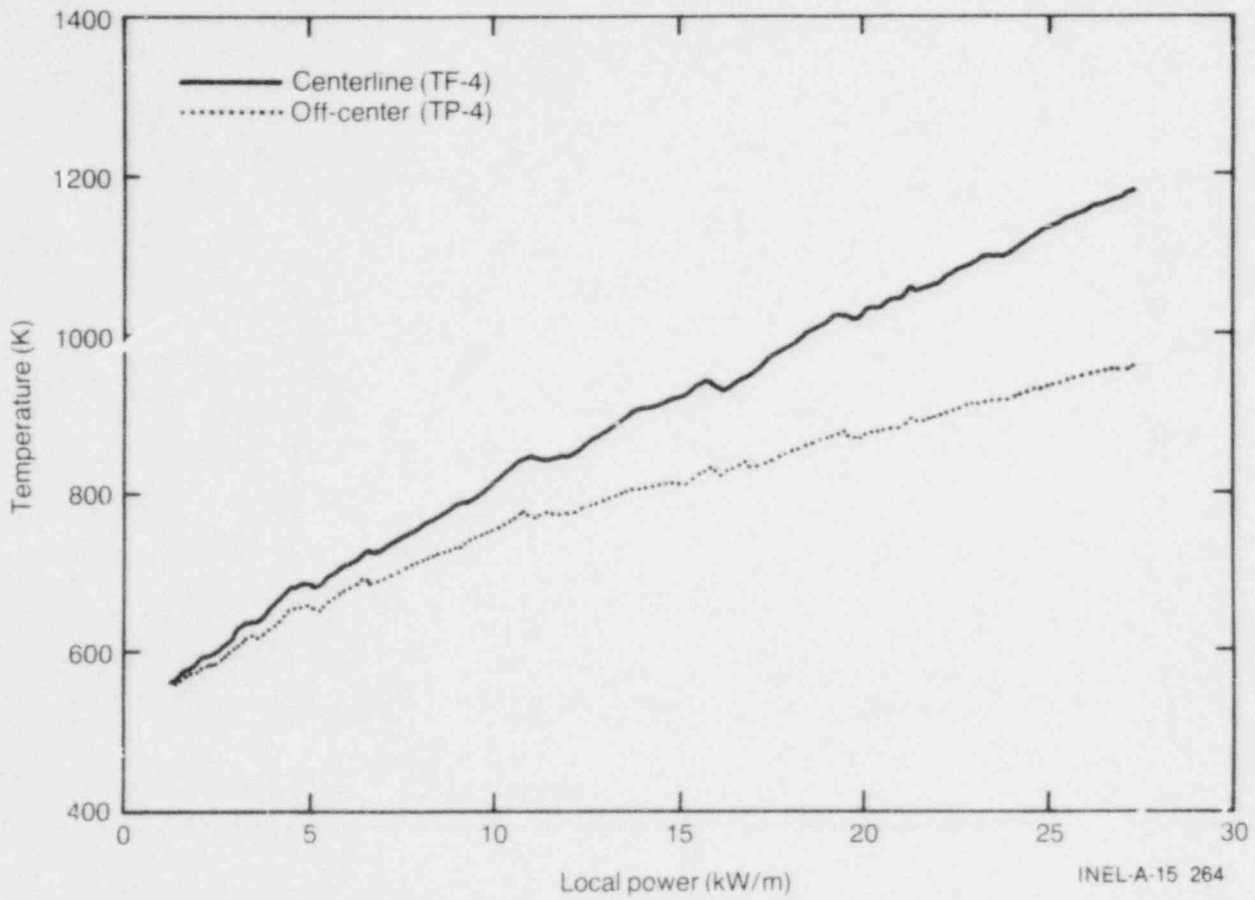


Figure 15. Lower centerline and one off-center temperature of small gap thermocouple rod (Rod 3) during first power ramp up.

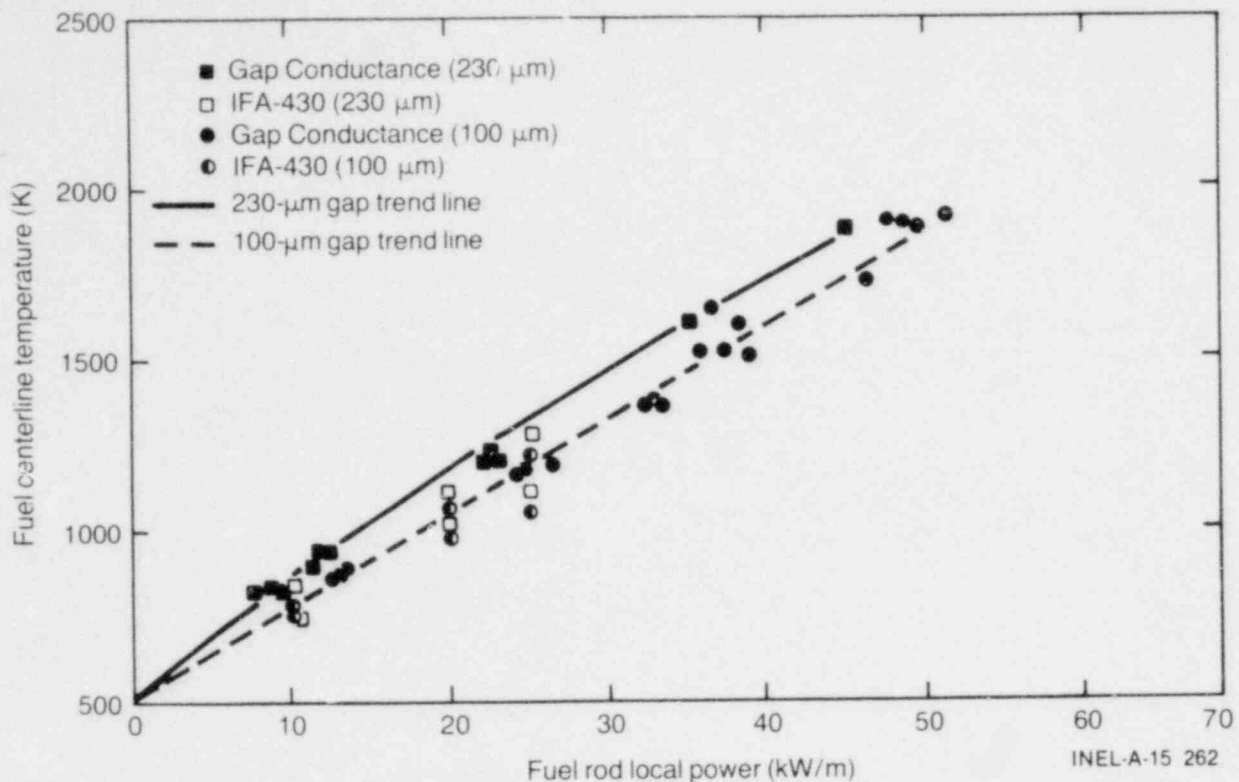


Figure 16. Comparison of fuel centerline temperatures measured in the Gap Conductance Tests with fuel temperatures measured in the IFA-430 Tests.

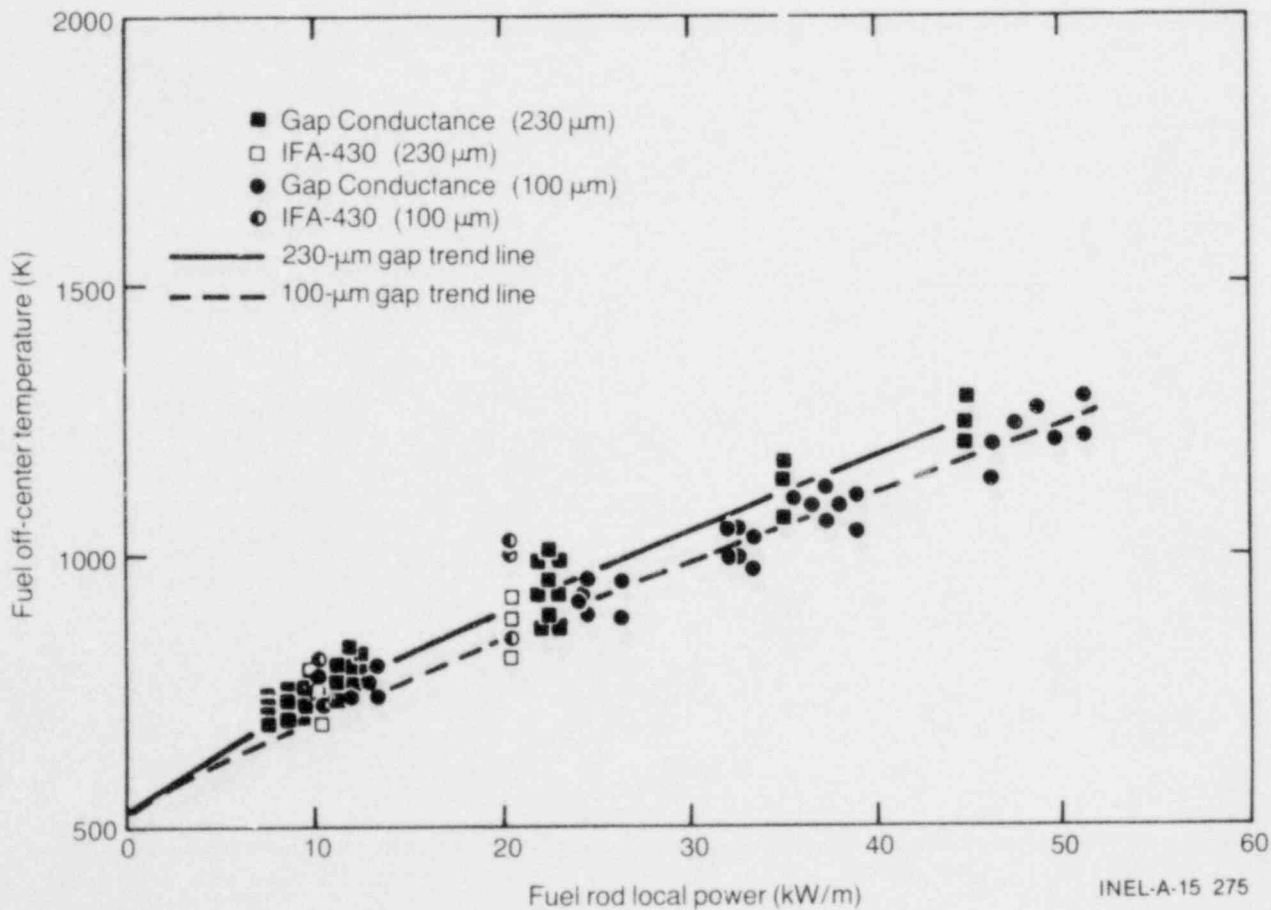


Figure 17. Comparison of fuel off-center temperatures measured in the Gap Conductance and IFA-430 Tests.

5. FUEL BEHAVIOR

The thermal performance of UO_2 pellet fuel is affected by the cracking of the fuel pellets and relocation of the pellet fragments into the fuel-cladding gap. The resultant fuel configuration governs the heat transfer within the fuel rod and, thus, the stored energy in the fuel. The stored energy in the fuel determines the thermal behavior of the fuel during reactor operational changes and significantly affects the fuel rod behavior during off-normal reactor transients. For these reasons, the fuel rod power at which the fuel cracks, the extent of the cracking, how the fuel relocates, and the power at which cracking and relocation are complete are important in modeling the behavior of the fuel, designing and conducting tests on the fuel, and operating the fuel commercially.

Two means for determining fuel cracking and relocation behavior are (a) using the axial gas flow characteristics of the fuel rod to indicate changes in the flow path (fuel stack geometry), and (b) using centerline and off-center fuel thermocouples to indicate changes in the thermal response of the fuel. In the following sections the cracking and relocation of the fuel in IFA-430 during its initial nuclear operation are discussed, using the results of axial gas flow and fuel temperature data. The cracking and relocation that occurred during the first power ramp are discussed first, followed by discussions of the cracking and relocation occurring during three subsequent power ramps.

5.1 Cracking and Relocation During the Initial Power Ramp

Cracking and relocation are believed to occur at low powers during the first power ramp the fuel is exposed to. The results from the IFA-430 tests show this to be the case; however, the results indicate that cracking and relocation continue to occur up to powers higher than theoretically expected. In addition, the results indicate that the ramp rate is a controlling factor in the cracking behavior.

As described in Section 3, the hydraulic diameter for the two gas flow rods is calculated using steady state and transient gas flow data. The

hydraulic diameter, D_H , calculated using steady state gas flow data from the first power ramp and the FRAP-T5⁶ calculated gap size are shown in Figure 18. Note the difference between the slopes of the hydraulic diameter and FRAP calculated gap size curves at powers below 15 kW/m during the up ramp. The model used in FRAP was chosen to calculate the gap size based only on fuel free thermal expansion. If the hydraulic diameter decrease (with power) was due solely to the expansion of the fuel pellets as they increased in temperature, the slopes of D_H versus power and FRAP gap size versus power would be the same. The difference in these two slopes, at powers below 15 kW/m during the up ramp, indicates that the fuel is cracking and relocating during this period. The agreement between the slopes of the D_H and FRAP gap size curves at powers above 15 kW/m during the up ramp and at all powers during the down ramp indicates that only very minor cracking and relocation are occurring during this period. The continued cracking up to 15 kW/m during the first ramp is not predicted theoretically.

The theoretically based⁷ threshold for fuel cracking, that is, the power at which the fuel pellet hoop stress exceeds the UO_2 fracture stress, is calculated to be ~ 5 kW/m. The theoretical maximum hoop stress and UO_2 fracture stress are plotted as a function of power in Figure 19. This graph shows that the fuel is expected to crack well before reaching a power level of 15 kW/m. Some insight is gained by comparing the average D_H for the combination of the top and middle sections with the D_H of the top and middle sections individually. The gas flow rod and associated power profile are shown in Figure 20.

The average D_H for the top and middle sections of the gas flow rods is shown in Figures 21 and 22, respectively. The normalized average section powers for the middle, top, and total (top plus middle) sections of the rods are 1.2, 0.9, and 1.0, respectively. The apparent threshold at which cracking is completed for the small gap rod appears to be ramp rate dependent. The threshold in the high power section (high ramp rate) is ~ 20 kW/m (Figure 22), and in the low power section is ~ 14 kW/m (Figure 21). The D_H of the two sections combined is averaged in Figure 18, which

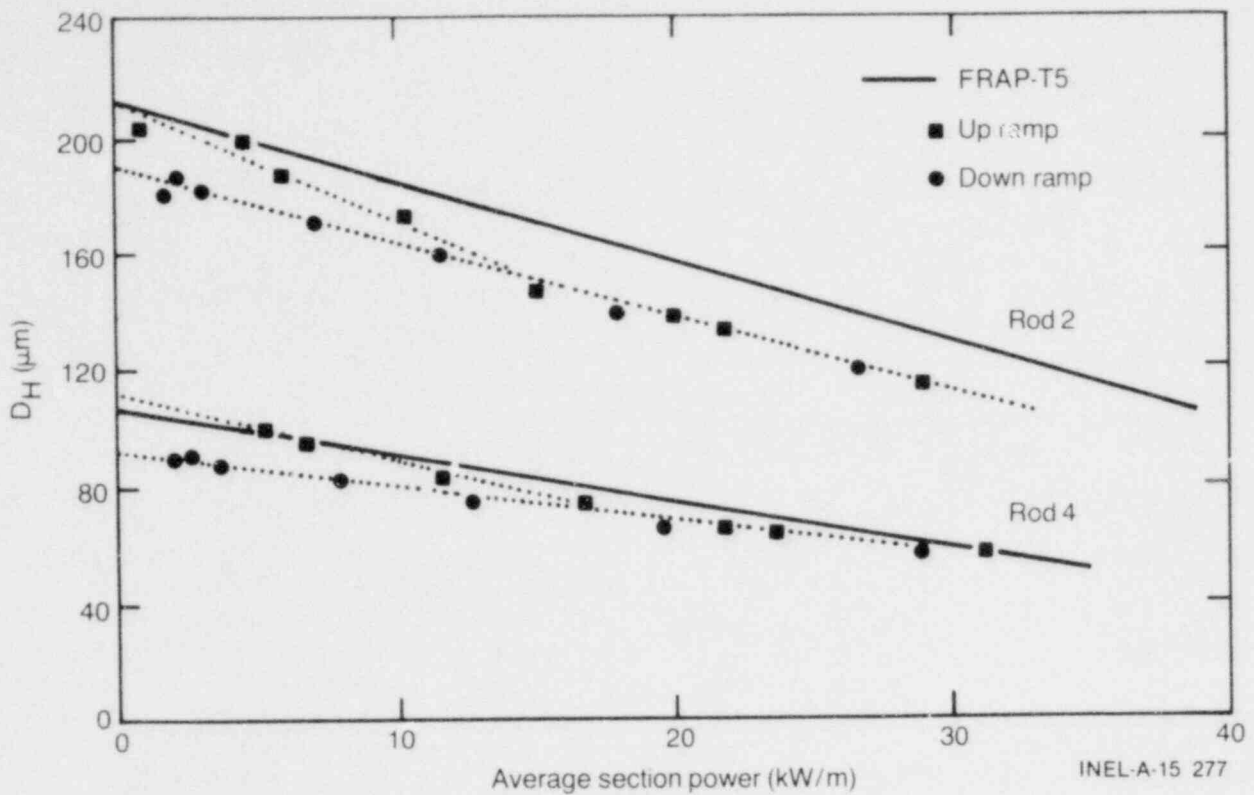


Figure 18. Average hydraulic diameter, D_H , for the total rod versus average rod power for the first power ramp up and down and FRAP-T5 calculated gap.

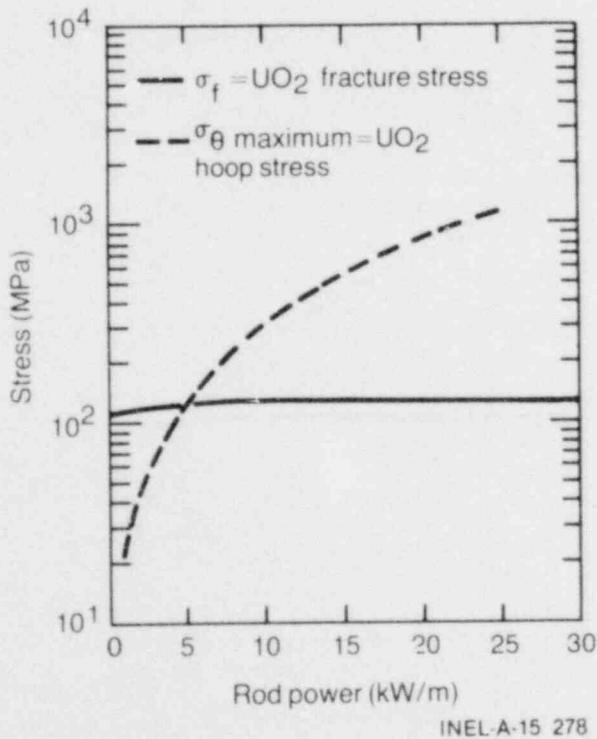


Figure 19. Hoop stress and UO_2 fracture stress as a function of power for IFA-430 design pellet.

shows a threshold at ~ 17 kW/m. Thus, it appears that the ramp rate may be affecting the cracking threshold. The average ramp rates during the first power ramp up for the top and middle sections of the small gap rod were 0.54 kW/m-h and 0.74 kW/m-h, respectively. In contrast to this apparent dependence of the cracking threshold on ramp rate is the effect of fabricated gap size.

The cracking threshold has a weak dependence on fabricated gap size. The two gas flow rods were fabricated with fuel-cladding diametral gap sizes of 100 and 230 μm . Comparison of the hydraulic diameter of the large and small gap rods for the top, middle, and total sections shows that the gap size has a mirror effect on the fuel cracking. The top (low power) section (Figure 21) of both rods shows only a small change in D_H , and the middle (high power) section (Figure 22) shows significant change in D_H for both large and small gap rods; yet the cracking threshold (change in slope) is essentially independent of the gap size, with only a slight bias to lower threshold as gap size increases.

Thus, it appears that the fuel begins cracking and relocating as power is increased during the

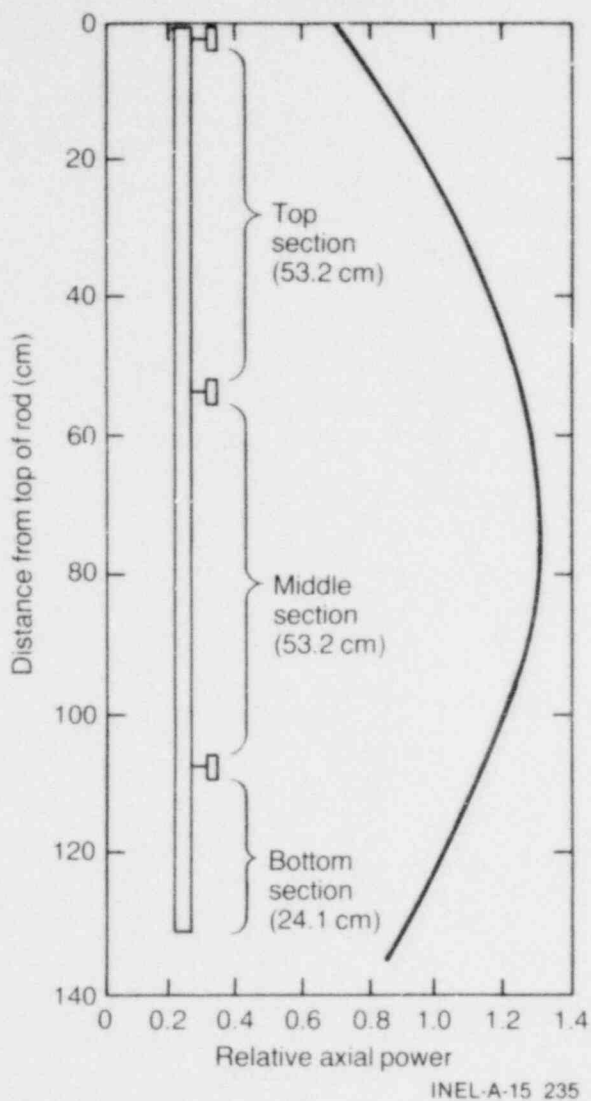


Figure 20. Gas flow rod sections and relative axial power profile for IFA-430 fuel rods.

first power ramp and continues cracking and relocating, with the cracking rate depending on the power ramp rate, up to a threshold power at which cracking and relocation is essentially complete. The cracking threshold shows only a weak dependence on fuel-cladding gap size; a larger gap size decreases slightly the power at which cracking is essentially complete. At powers higher than the cracking threshold, the hydraulic diameter changes agree well with those predicted by fuel free thermal expansion, indicating that cracking and relocation are essentially complete.

The fuel centerline temperatures in the two gas flow rods during the first power ramp up, shown

in Figures 13, 14, 23 and 24, indicate that at the thermocouple location some relocation occurs at ~ 19 kW/m. The relocation appears to occur between 38 and 40 h (Figure 24) during the steady power period. This corresponds approximately to the power at which the gas flow data (Figures 21 and 18) indicate cracking and relocation are complete. Thus, both the gas flow and fuel temperature data for the small gap gas flow rod indicate that fuel cracking and relocation are occurring at powers up to ~ 19 kW/m.

5.2 Cracking and Relocation Following the Initial Power Ramp

The major cracking and relocation of UO_2 pellet fuel (during early life) is shown to occur during the first power ramp the fuel experiences. The gas flow data and fuel temperature measurements show that only minor additional cracking or relocation, or both, occur during the second, third, and fourth power ramps. Figure 25 presents the hydraulic diameter at zero power for the first four power ramps. These data were calculated by performing a least squares fit of the hydraulic diameter data from each of the power ramps and using the fitting equations to calculate the zero power D_H value. Figure 25 shows that for both the large and small gap gas flow rods, the significant change in the hydraulic diameter occurs during the first power ramp and, as discussed in the previous section, during the up ramp, with only very minor relocation occurring during subsequent ramps. This trend is supported by the fuel temperature data.

It is expected that as cracking and relocation occur, the fuel centerline temperature will be affected. For radial (diametral) cracks, the fuel centerline temperature is expected to decrease due to the decreased gap width that results from the fuel relocating into the gap. Circumferential cracks decrease the fuel effective thermal conductivity and thus increase the fuel centerline temperature. The IFA-430 data show decreasing or unchanging fuel centerline temperature with subsequent power ramps, indicating that radial cracking is occurring. In Figure 26, the fuel centerline temperature of the upper section (no off-center thermocouples) of the small gap thermocouple rod at 10 and 20 kW/m is shown as a

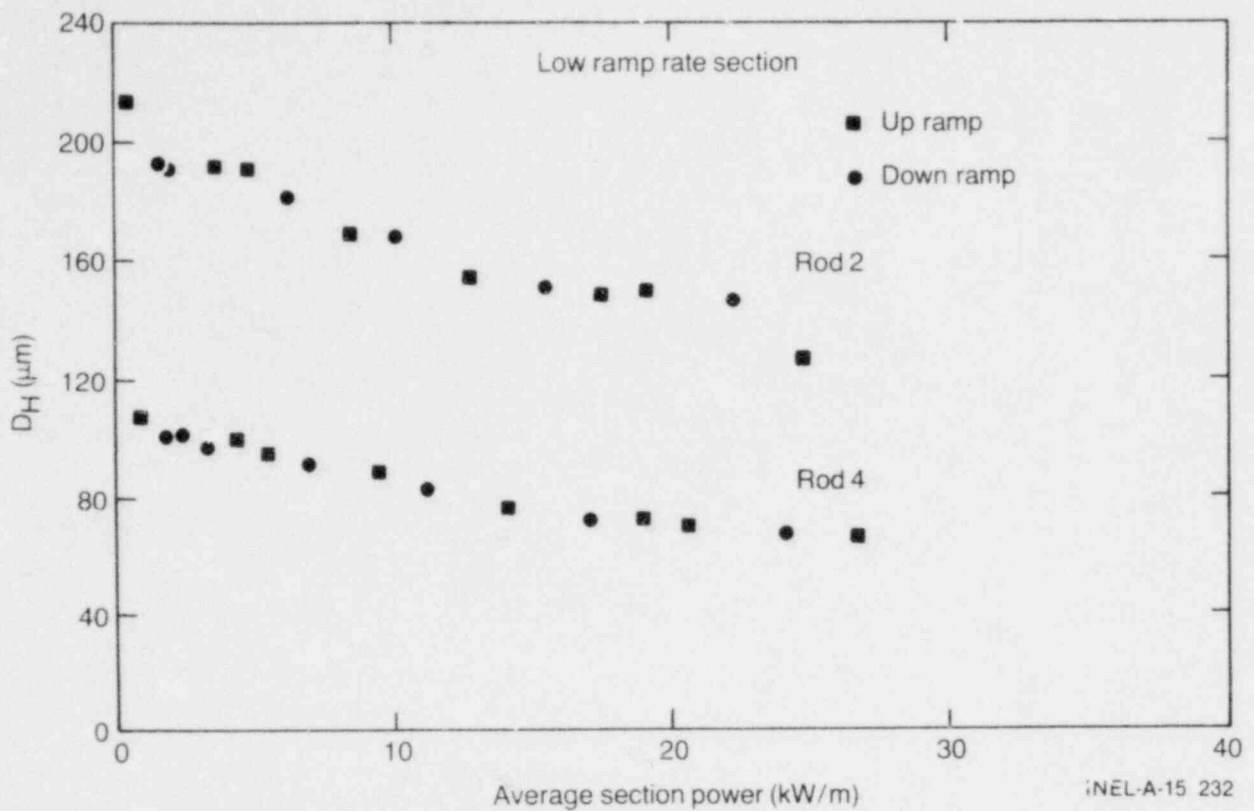


Figure 21. Average hydraulic diameter, D_H , of the top section of Rods 2 and 4 as a function of section average power for the first power ramp up and down.

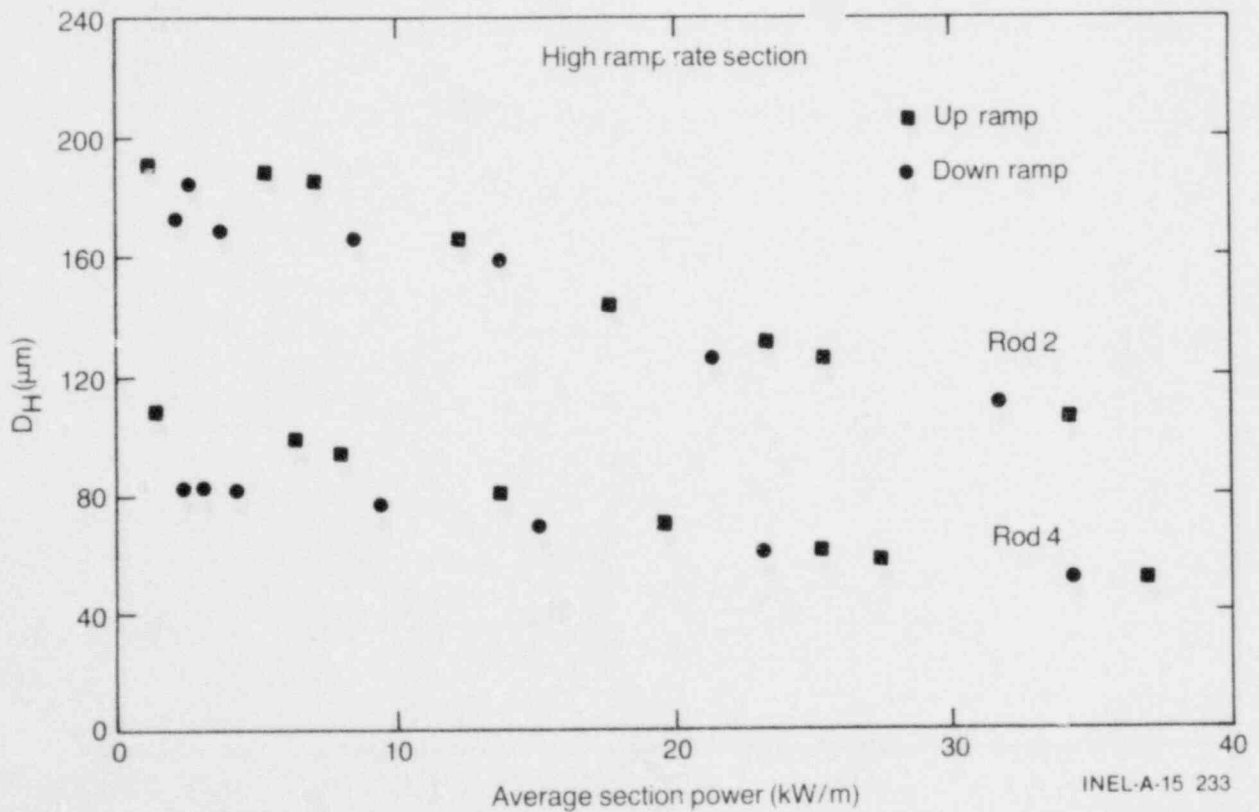


Figure 22. Average hydraulic diameter, D_H , of the middle section of Rods 2 and 4 as a function of section average power for the first power ramp up and down.

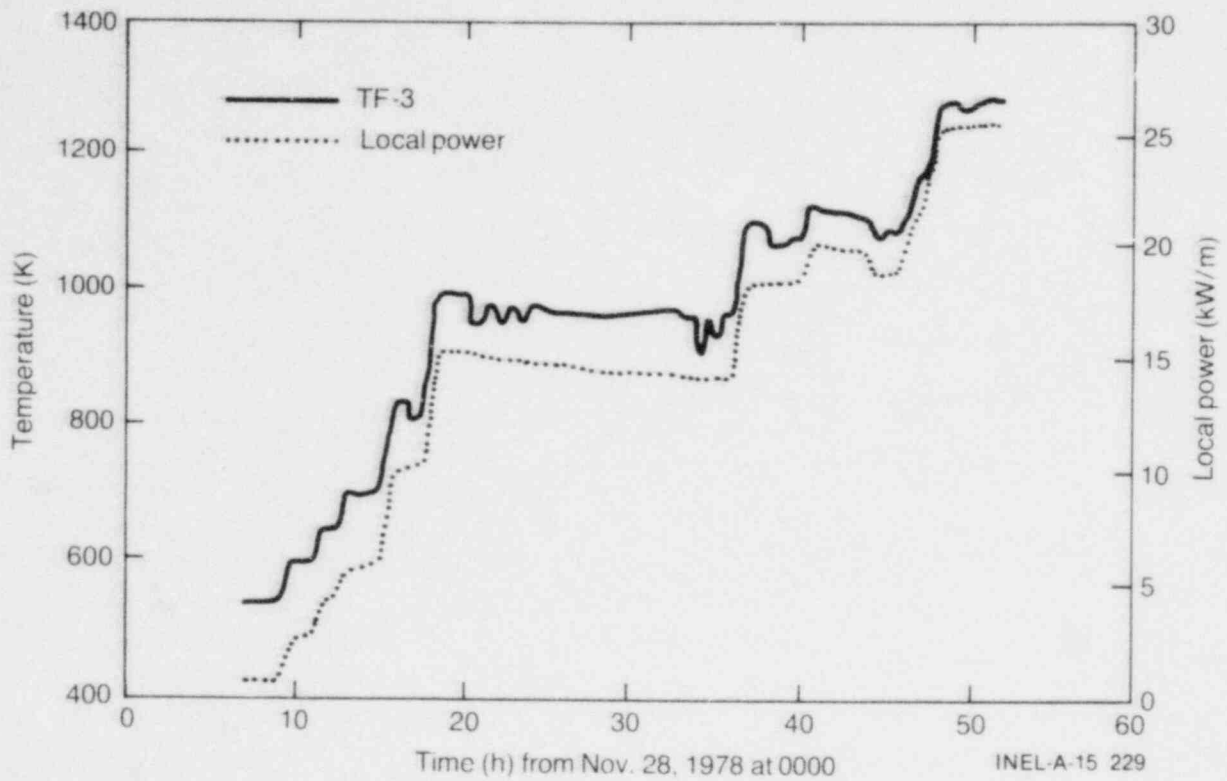


Figure 23. Lower centerline temperature and local power of large gap gas flow rod (Rod 2) during first power ramp up.

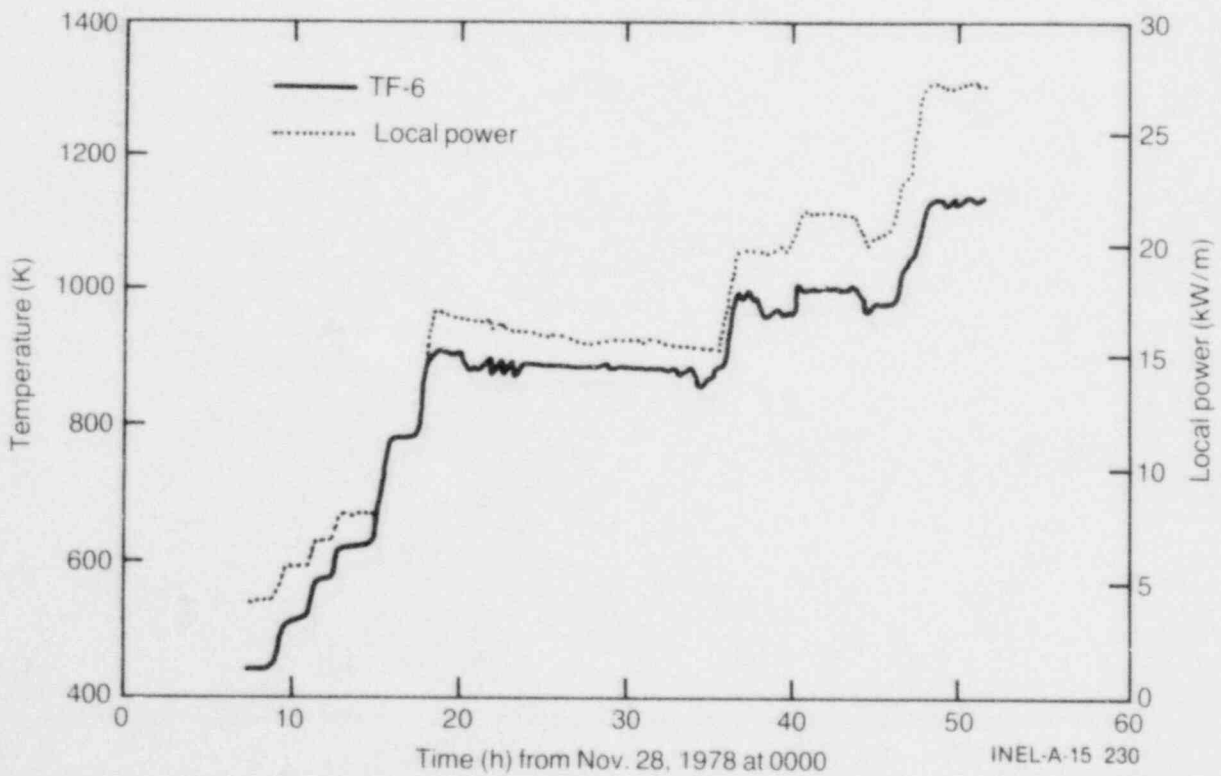


Figure 24. Centerline temperature and local power of small gap gas flow rod (Rod 4) during first power ramp up.

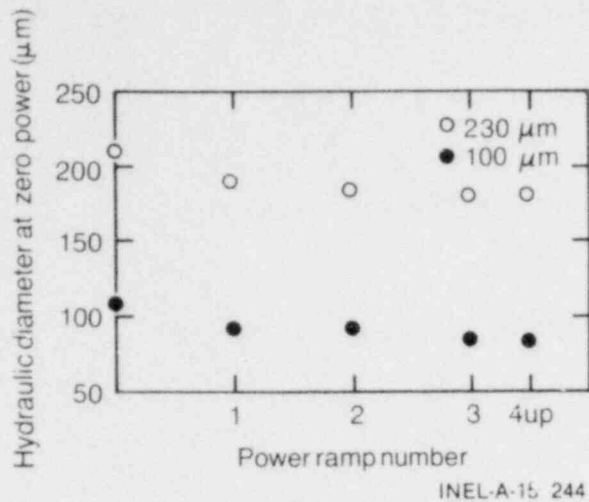


Figure 25. Hydraulic diameter extrapolated to zero power for the first four power ramps and prior to irradiation.

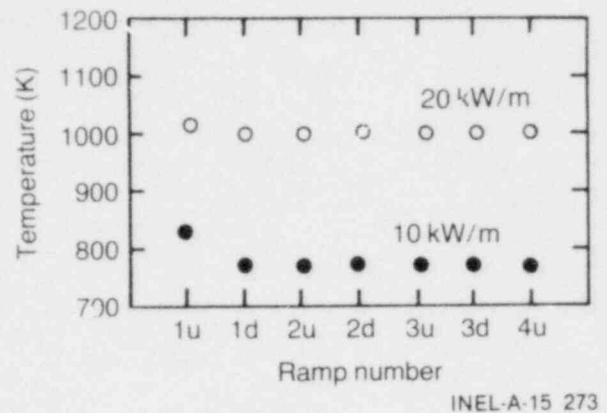


Figure 26. Upper centerline temperature of small gap thermocouple rod (Rod 3) at 10 and 20 kW/m local power during each power ramp.

function of ramp number. Note that the significant change in temperature occurs in the first power ramp up between 10 and 20 kW/m, shown in detail in Figure 27, and that during the following ramps no significant change occurs. The data shown in Figures 25 and 26 indicate that radial cracking and relocation of the fuel are occurring during the first ramp up, and that on subsequent ramps very little, if any, further cracking occurs.

Cracking and relocation appear to occur predominantly during the first power ramp up, below a threshold power level that is strongly dependent on ramp rate and weakly dependent on fabricated fuel-cladding gap size. During subsequent power ramps, there is no indication from the gas flow or fuel temperature data of further cracking, crack healing, or relocation.

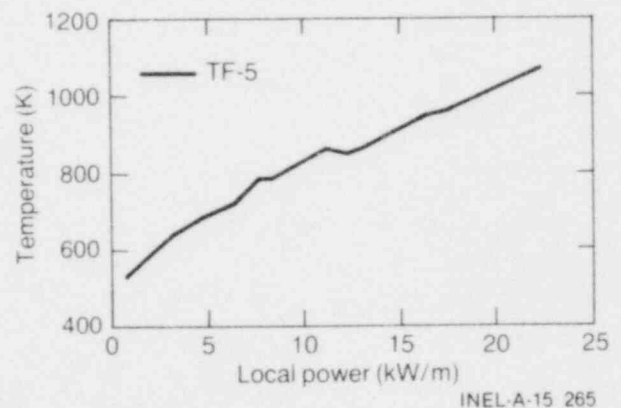


Figure 27. Upper centerline temperature of small gap thermocouple rod (Rod 3) during first power ramp up.

6. CONCLUSIONS

Analysis of the fuel temperature and axial gas flow data obtained during startup of the Halden IFA-430 experiment supports the following conclusions regarding the cracking and relocation of UO_2 pellet fuel during initial nuclear operation.

1. The fuel begins cracking as the power is increased during the first power ramp and continues cracking, with the cracking rate depending on the power ramp rate, up to a threshold power at which cracking is essentially complete. The cracking threshold (power) shows a weak dependence on fuel-cladding gap size; a larger gap size decreases slightly the power at which cracking is essentially complete. At powers above the cracking threshold power, the fuel mechanical behavior agrees with that predicted by free thermal expansion, indicating that no further significant cracking and relocation are occurring.
2. The cracking and relocation during the first ramp continue up to powers higher than theoretically predicted. For the IFA-430 fuel design, cracking is theoretically predicted to occur at powers of ~ 5 kW/m; the data show that significant cracking continued to occur up to powers of 15 to 20 kW/m.
3. The hydraulic diameter for axial gas flow, which is an indicator of fuel cracking and relocation changes, and the fuel centerline and off-center temperatures show no evidence of significant cracking and relocation occurring during the second, third, or fourth power ramp, nor is there any indication of crack healing.

7. REFERENCES

1. United States Nuclear Regulatory Commission, Division of Reactor Safety Research, *Water Reactor Safety Research Program—A Description of Current and Planned Research*, NUREG-0006, February 1979.
2. S. J. Dagbjartsson et al., "Investigations on Axial Gas Flow Within High Burnup Fuel Rods," *Proceedings of ANS Topical Meeting on Thermal Reactor Safety, Sun Valley, Idaho, July 31-August 4, 1977*.
3. E. Karb et al., *Theoretische und Experimentelle Untersuchungen zur Gasstromung in LWR Brennstäben bei Kühlmittelverlustfällen*, Kernforschungszentrum Karlsruhe, KfK-2411, December 1976.
4. R. W. Garner et al., *Gap Conductance Test Series-2, Test Results Report for Tests GC 2-1, GC 2-2, and GC 2-3*, NUREG/CR-0300, TREE-1268, November 1978.
5. M. Reimann, *Analytische Untersuchung von Gasströmungen in Ringspalten beim Aufblähvorgang von Zirkaloy-Hüllrohren*, Kernforschungszentrum Karlsruhe, KfK-2280, Part 1, May 1976.
6. L. J. Siefken et al., *FRAP-T5—A Computer Code for the Transient Analysis of Oxide Fuel Rods*, NUREG/CR-0840 TREE 1281, June 1979.
7. D. R. Olander, *Fundamental Aspects of Nuclear Reactor Fuel Elements*, TID-26711-P1, 1976.



EG&G Idaho, Inc.
P.O. Box 1625
Idaho Falls, Idaho 83415